RESEARCH

Spatial assessment of soil erosion by water using RUSLE model, remote sensing and GIS: a case study of Mellegue Watershed, Algeria–Tunisia

Okba Weslati · Mohamed-Moncef Serbaji

Abstract Soil erosion is an important global phenomenon that can cause many impacts, like morphometry and hydrology alteration, land degradation and landslides. Moreover, soil loss has a significant effect on agricultural production by removing the most valuable and productive top soil's profile, leading to a reduction in yields, which requires a high production budget. The detrimental impact of soil erosion has reached alarming levels due to the exacerbation of global warming and drought, particularly in the arid climates prevalent in Tunisia and Algeria and other regions of North Africa. The influence of these environmental factors has been especially evident in the catchment of Mellegue, where profound vegetation loss and drastic changes in land use and cover, including the expansion of urban areas and altered agricultural practices, have played a significant role in accelerating water-induced soil loss between 2002 and 2018. The ramifications of these developments on the fragile ecosystems of the region cannot be overlooked. Accordingly, this study aimed to compare

soil losses between 2002 and 2018 in the catchment of Mellegue, which is a large cross-border basin commonly shared by Tunisian–Algerian countries. The assessment and mapping of soil erosion risk were carried out by employing the Revised Universal Soil Loss Equation (RUSLE). This widely recognised equation provided valuable insights into the potential for erosion. Additionally, changes in land use and land cover during the same period were thoroughly analysed to identify any factors that may have contributed to the observed risk. By integrating these various elements, a comprehensive understanding of soil erosion dynamics was achieved, facilitating informed decision-making for effective land management and conservation efforts. It requires diverse factors that are integrated into the erosion process, such as topography, soil erodibility, rainfall erosivity, anti-erosion cultivation practice and vegetation cover. The computation of the various equation factors was applied in a GIS environment, using ArcGIS desktop 10.4. The results show that the catchment has undergone significant soil water erosion where it exhibits the appearance of approximately 14,000 new areas vulnerable to erosion by water in 2018 compared to 2002. Average erosion risk has also increased from 1.58 t/ha/year in 2002 to 1.78 in 2018, leading to an increase in total estimated soil loss of 54,000 t/ha in 2018 compared to around 25,500 t/ha in 2002. Maps of erosion risk show that highly eroded areas are more frequent downstream of the basin. These maps can be helpful

O. Weslati (✉)
Laboratory of Water, Energy, Environment, National Engineering School of Sfax (ENIS), University of Sfax, Sfax, Tunisia
e-mail: Okba.weslati@gmail.com

M.-M. Serbaji
Laboratory for Environmental Engineering and Eco-Technology, National Engineering School of Sfax (ENIS), University of Sfax, 3038 Sfax, Tunisia

for decision-makers to make better sustainable management plans and for land use preservation.

Introduction

Water erosion is a global phenomenon that seriously hinders sustainable development. The physical processes that govern this phenomenon are directed by different factors such as climate, topography, soil texture, hydrology and vegetation cover (BACC II Author Team, 2015; Ciampalini et al., 2012; Durán Zuazo et al., 2005; Littleboy et al., 1992; Negese, 2021; Nunes et al., 2010). The main agents of water erosion are precipitation and runoff. Combined with the effect of gravity, they provide the required dynamism for the detachment and transport of soil particles. The aggressiveness of erosion depends essentially on the quantity and duration of the water action on the soil, while the vulnerability of the soil to erosion depends on its texture, structure and ability to infiltrate (Guerra, 1994; Ostertagová, 2012; Wang et al., 2021).

In the semi-arid Mediterranean environment, water erosion is very active and has manifested itself in several forms (Biswas, 1990; Gebregziabher et al., 2016; López-Bermúdez, 1990; Prosdocimi et al., 2016; Raclot et al., 2018; Shalaby & Tateishi, 2007; Zema et al., 2022); laminar (or random) sheet erosion is a form of diffuse erosion; it represents the initial stage of soil degradation by erosion and is slightly distinguished from 1 year to the next. Linear erosion is a form of loss created by streams. It occurs when the soil reaches its maximum capacity of infiltration from rainfall, generating communicating puddles with each other through the streams of water, which acquire a certain speed and energy capable of triggering local erosion along flow lines. Mass erosion defines the movement of the superficial layers of the soil cover. It contains all kinds of landslides, including mass movements, landslides or even mudslides. It is caused by an imbalance created between the mass of the soil cover and the amount of water stored, as well as the vegetation occupancy on the surface. Another special form of erosion generally occurs through the action of the energy of streams or rivers on their beds. The

energy created can wash away the edges of rivers, which is often observed in the meanders of streams, more precisely on the concave side of the river's bed.

Regardless of the nature of the erosion, the associated impacts of this phenomenon are innumerable (Gilley, 2005; Sergieieva, 2021). The consequences include the degradation of the agricultural landscape and the siltation of hydro-agricultural infrastructure. In addition to the degradation of water quality, water erosion can cause significant damage to agricultural crops. When the quantity of sediment lost by erosion exceeds the rate of natural soil regeneration (usually very slow), the soil loses its fertility and becomes less dense. Studies of the impact of water erosion on land fertility should be carried out over a period of 20 to 25 years (Morgan, 2005). Generally, the global soil erosion rate stands at an average of 2.4 t/ha/year, whereas the estimated average country discontinuity sits at 1.4 t/ha/year (Wuepper et al., 2019). However, it should be noted that tolerance depends on the economic and environmental issues of each region. As far as the quality of river water is concerned, it will depend on the concentration of suspended solids in the watercourse. Water erosion can bring changes in agricultural cover as it provides particle size selectivity where the finer particles are moved far down slopes while the coarse particles are near their erosion sites. This process allows sorting and redistribution of eroded materials, which can have considerable agronomic and environmental repercussions in agricultural environments.

As for watersheds, the environmental damage caused by water erosion is numerous (Biswas, 1990; Cooper, 2010; Gebregziabher et al., 2016; Mohanty, 2016; Pavlova-traykova, 2020; Sbai et al., 2021; Singh, 1989; Starr et al., 2000; Vezina et al., 2006). The eroded particles rich in fine mineral and organic fractions will be transported and deposited to make a chemical enrichment in nutrients used frequently in agriculture (phosphorus and nitrogen). The consequences are noticed in the loss of soil fertility and the decrease in crop yield. The watercourses will also be contaminated by the transported sediments, which can pose risks of toxicity for the fauna and flora. The fine particles that are in suspension will increase the turbidity of the water and minimise their penetration, which constitutes a favourable environment for eutrophication and siltation of water bodies. Erosion and sedimentation constantly modify the morphology of rivers. Transported sediments that raise tributary

beds will disable navigation and could increase the risk of flooding. In addition, another widespread phenomenon of water erosion occurs in the siltation of reservoirs. These structures will end up weakening over time and will lose some storage as a result. That is why water structures require continuous development and an extra cost of maintenance.

A study of the temporal and spatial distribution of water erosion is essential at the watershed scale. It is therefore essential to opt for conventional methods of evaluating water erosion and sediment conveyance in order to better manage the problems associated with this phenomenon. Modelling proves to be such a reliable tool for quantifying soil losses due to the adopted universal models (Aiello et al., 2015; De Jong et al., 1999; Khemiri & Jebari, 2021; Touai'bia et al., 1999; Wasswa & Olilla, 2006). This approach will be used later for decision-making and effective management of water and soil resources. Various empirical and statistical models have been applied particularly to the study of water erosion. The choice of adequate model depends on the purpose and suitability of the local conditions in the study area as well as the availability of data. The Revised Universal Soil Loss Equation (RUSLE) approach is an invaluable tool for estimating soil loss and plays a crucial role in sustainable land management. This empirical and spatialised model offers a systematic framework for quantifying the rate of soil erosion and predicting its potential impact on land resources. To fully harness the power of the RUSLE model, it is imperative to couple it with a geographic information system (GIS) to integrate RUSLE factors. This combination enables a more comprehensive understanding of the spatial distribution and intensity of soil erosion, aiding in the implementation of effective soil conservation measures (Kebede et al., 2021).

The RUSLE approach takes into account various factors that contribute to soil erosion, including rainfall erosivity (R), soil erodibility (K), slope (LS), land cover (C) and erosion control practices (P). By considering these variables, the model provides a holistic assessment of soil loss potential and guides resource managers and policymakers in making informed decisions regarding soil conservation practices (Thapa, 2020).

The integration of the RUSLE model with GIS technology enhances its capabilities by incorporating spatial data analysis and visualisation. GIS allows for the creation of detailed soil erosion risk maps, which depict areas of heightened vulnerability to erosion. These maps can be used to prioritise resource allocation, identify critical erosion hotspots and develop targeted soil conservation strategies. GIS also facilitates the implementation of real-time monitoring systems, enabling land managers to track changes in soil erosion patterns and assess the effectiveness of conservation measures over time.

One of the key advantages of using the RUSLE model coupled with GIS is its applicability to a wide range of landscapes and scales. Whether it is assessing erosion risks in agricultural fields, forested areas or urban environments, the model can be tailored to suit diverse land use scenarios. This versatility makes it an invaluable tool for land managers, researchers and policymakers involved in soil conservation efforts across various sectors (Allafta & Opp, 2022; Kebede et al., 2021; Sidi Almouctar et al., 2021).

Furthermore, the integration of the RUSLE model with GIS promotes data-driven decision-making in soil erosion management. By incorporating real-time monitoring data, satellite imagery and other geospatial information, stakeholders can make informed choices about the most effective erosion control practices for specific locations. This targeted approach optimises resource allocation, minimises costs and maximises the long-term sustainability of land resources.

In conclusion, the RUSLE approach, when integrated with a GIS, offers a powerful tool for estimating soil loss and guiding soil conservation efforts. By considering key factors contributing to erosion, the model provides valuable insights into soil erosion risks and aids in the development and implementation of effective conservation strategies. The combination of the RUSLE model and GIS technology enables spatial data analysis, visualisation and real-time monitoring, facilitating data-driven decision-making in soil erosion management. With its versatility and applicability across diverse landscapes, this approach has the potential to contribute significantly to sustainable land management practices and the protection of our vital soil resources.

This study is a multi-temporal analysis of the erosion loss in the Mellegue watershed. It consists of comparing 2002 and 2018 sediment loss in the catchment and studying associate factors for any potential rate change. The spatial distribution of erosion will be presented in the form of thematic maps, presenting the results of analysis of different factors involved in

the process as well as the production of maps showing the annual erosion rate and exhibiting the most vulnerable areas to this phenomenon.
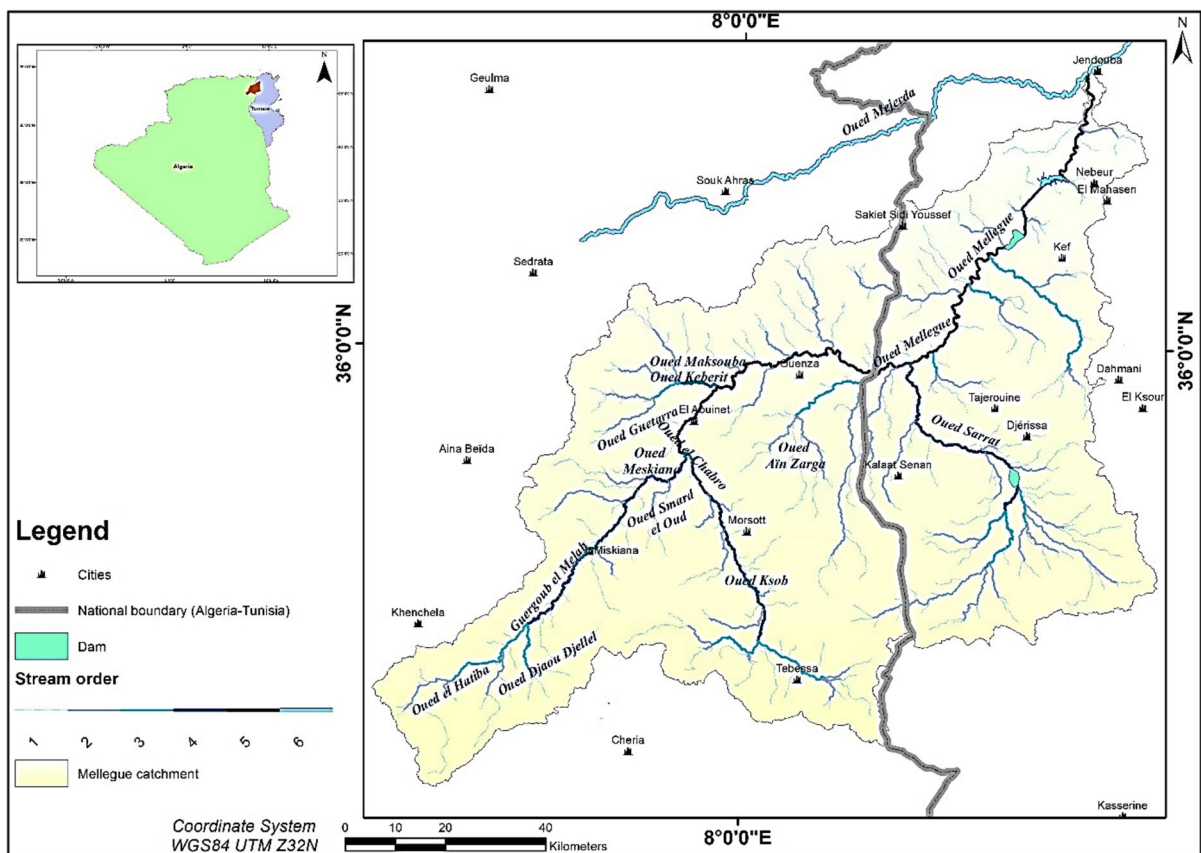
Study area

The Mellegue watershed is located between 35.21°, 36.43° North and 7.19°, 8.92° East. It is a sizable cross-border catchment, occupying an area of more than 1 million ha and 1054 km of perimeter (Fig. 1). 625,500 ha of that area (60%) is part of Algeria, while the rest of the area, along with the outlet, belongs to Tunisia. The mainstream of the watershed is called Oued Mellegue. It originates in Algeria, starting from the mounts of Tebessa through the famous Aures massif of Algeria (Belloula & Dridi, 2015). It flows in Tunisia, through the Tunisian Atlas, until it finally unclogs into the river Mejerdah, near Jendouba. The overall direction of the river matches the

southwestern-northeastern direction of the famous Algero-Tunisian Atlas (Weslati et al., 2020, 2023). The watershed is characterised by an elongated overall shape, is oriented NE-SW and is explicitly large in the middle. The slope of the catchment is generally low to moderate, and 70% of the study area defines a low slope relief (near 3%). In contrast, strong slope relief occupies only 3% of the total area.

The geology of the catchment is complex and defines an assortment of ages that extends from Triassic to Quaternary, with the exclusion of Jurassic deposits. The region is also known for multiple evaporitic outcrops due to Triassic salt extrusions through border faults. The structural feature of the area reveals complicated forms such as the NE-SW folds that define the diapiric zone near the Algero-Tunisian boundary, the famous Atlasic sector or the Neogene folds (Rouvier, 1977).

Sparse vegetation cover occupies most of the basin. The mountains generally hold varied vegetation,

Fig. 1 Location of study area

while the foothills are nearly undeveloped and the plains are often farmed. The thickest forests are infrequently present, locally spotted downstream of the basin. Contrariwise, cultivated and bare lands are frequently widespread, covering most of the watershed's area (Rodier et al., 1981).

The catchment is known for its arid to semi-arid climate, which is exceptionally subhumid on the north border. It is generally distinguished by moderate winters (humid) and hot summers (dry). Rainfalls are too sensitive within the catchment and explicitly specific to each region. Yearly rainfalls generally vary from 450 to more than 750 mm/year. The mean yearly temperature fluctuates around 16°C, where seasonal maximum and minimum temperatures go near 39°C (± 3°C) and 3°C (± 4°C), respectively. The lowest temperatures are mostly recorded in the west and in the north of the basin, where it often snows (Belloula, 2017).

Materials and data

This work is based on the application of the RUSLE model integrated into a GIS environment for the mapping, quantifying and evaluating of water erosion in the Mellegue watershed for the dates 2002 and 2018. This comparative approach makes it possible to see the spatial distribution and the spread of erosion through the entire catchment.

The Revised Universal Soil Loss Equation

It was first introduced by Renard et al. (1976). It defines an improved version of the USLE model. The enhancement made the equation more suitable for new generations of models that use RUSLE as an empirical process for quantifying soil erosion. The model is based on the same USLE equation while conceiving new methods to evaluate the associated factors. These new methods take into consideration quantitative data on the seasonal variation of the resistivity factor (K), the impact on erosion, crop management (C factor) and even the relationships between irregular slopes (LS factor). The computation of the RUSLE model requires a database that provides information on the erodibility of the soil (K factor), on the climate (R factor) and on the various known soils in the world.

The equation used for estimating soil losses is the same for the RUSLE and USLE models. It is expressed by the following relationship:

$$A = R \times K \times \mathrm{LS} \times C \times P$$

While:

A (t/ha/year): is the rate of potential annual losses. The results obtained can later be compared to the tolerable land loss thresholds in order to assess the risk of erosion.

R (MJ mm/ha/h/year): constitutes the rain erosivity factor for a given geographical area. The greater the intensity and interval of precipitation, the greater the risk of erosion.

K (t/h/ha/MJ/mm): represents the erodibility of the soil and depends on several soil characteristics such as texture, richness in organic matter, permeability *and structure*.

LS: combines the length of the slope (L in m) and its inclination (S in %). By analogy, high erosion risk is directly influenced by long and/or steep slopes.

C: corresponds to the plant cover factor, with the exception of bare soil, and is under the direct influence of human activity, which can greatly increase the risk of erosion.

P: expresses an anti-erosion development factor that depends on agricultural practices and soil conservation.

Methodology and settings of the RUSLE model

RUSLE model factors were estimated based on annual precipitation, digital terrain model (DEM), soil type and land cover. The methodology adopted in this study is schematised in the following figure (Fig. 2).

To estimate annual precipitation, historical climatic data from reliable sources were collected and analysed. These data included precipitation values for each month over a specified time period. By considering the temporal patterns and spatial distribution of precipitation, accurate estimates were obtained.

Incorporating the DEM was crucial to understanding the topographic characteristics of the study area. DEM data provided valuable insights into slope, aspect and elevation, which influenced erosion potential. Advanced techniques, such as GIS, were employed to accurately process and analyse the DEM information.
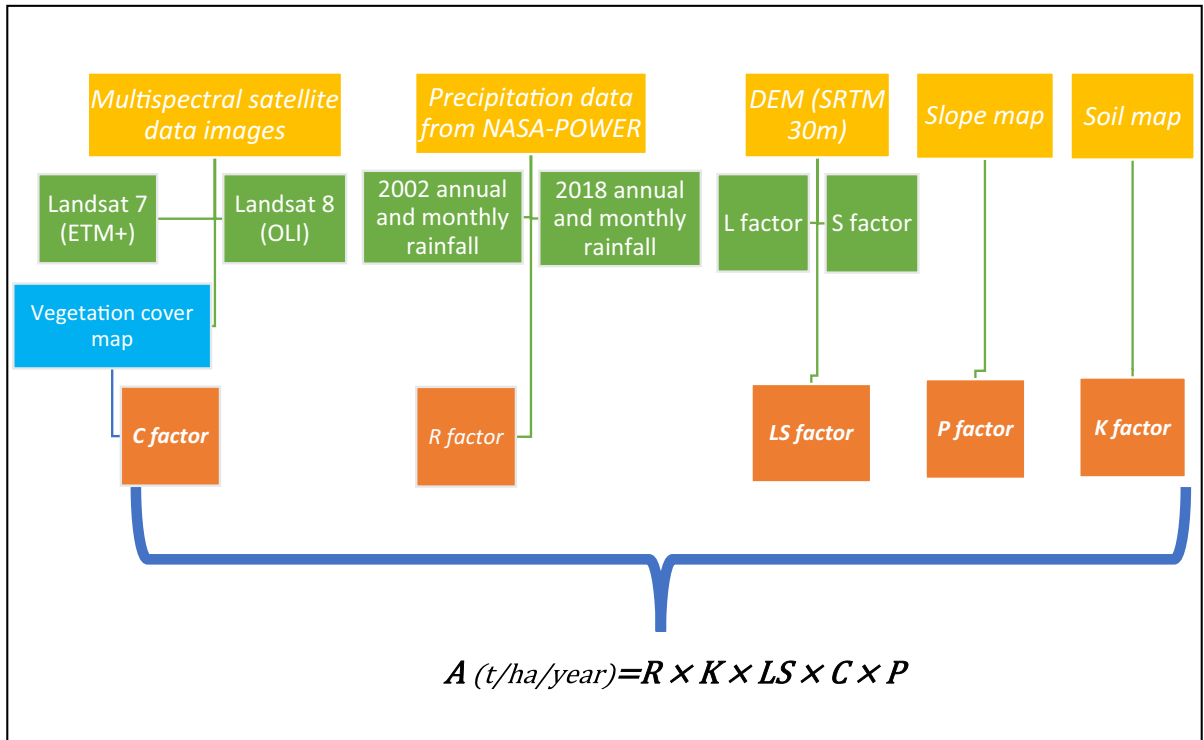
Fig. 2 Applied methodology for this study

Soil type played a significant role in determining erosion rates within the RUSLE model. Extensive field surveys were conducted to collect soil samples for laboratory analysis. The soil properties, including texture, organic matter content, permeability and cohesion, were examined to determine their erosional susceptibility. These findings were then integrated into the RUSLE model.

Land cover was another essential factor in assessing erosion potential. Remote sensing techniques, combined with satellite imagery, originally taken from Landsat 7 of ETM+and Landsat 8 of OLI for 2002 and 2018, respectively, were utilised to classify and quantify the land cover in the study area. This information provided valuable data on vegetation density, land use changes and soil exposure, which were directly linked to erosion rates.

In conclusion, this study employed a professional and rigorous approach to estimate RUSLE model factors. By incorporating annual precipitation, DEM, soil type and land cover, a comprehensive understanding of erosion potential was achieved. These findings will contribute to informed decision-making and sustainable land management practices for a wide range of stakeholders.

Rainfall erosivity factor

The R factor describes the susceptibility of rainfall to initiate erosion at a particular location, depending mainly on the amount and intensity of precipitation. It reflects the effect of rainfall intensity on soil erosion. This factor is used in the RUSLE model to quantify precipitation and its impact. It is expressed in megajoule millimetres per hectare per hour per year (MJ mm/ha/h/year), and it computes the amount and rate of runoff associated with rainfall events. Since data related to kinetic energy and rainfall intensity are complex and difficult to find, there are various formulas that implement daily and monthly precipitation for R factor calculation. The integral equation to generate the factor R has been used by different researchers in Morocco and Tunisia, according to the specific erosive features of the North African region (Khanchoul et al., 2020; Sadiki et al., 2004):

$$R = 143 \times \log\left(P \times P_{24}^2 \times 10^{-6}\right) + 89.7$$

Where R is the erosivity factor (MJ mm/ha/h/year); P is the average annual precipitation (mm/year); and P_{24} is the median maximum rainfall (mm) for 24 h for the considered year.

Rainfall data was obtained from the assimilation model products of Goddard's Global Modelling and Assimilation Office (GMAO)'s Modern Era Retrospective-Analysis for Research and Applications (MERRA-2). These simulation results provide valuable insights into global precipitation patterns. The MERRA-2 data cover a significant time range, starting in 1981 and extending to a few months ahead of the current time. To ensure accuracy and consistency, the MERRA-2 simulation results were compared and interpolated with another reliable simulation model, GEOS 5.12.4. This comparison revealed a high degree of similarity between the two models, minimising any potential discontinuities that are often observed in different assimilation models. The worldwide grid used in this study contains comprehensive information about precipitation distribution across the globe. This data allows researchers and scientists to analyse rainfall patterns on both regional and global scales, providing crucial insights into climate dynamics and variability. By utilising advanced assimilation techniques, the MERRA-2 dataset is able to capture fine-scale details of rainfall events, enabling accurate and detailed analysis.

The assimilation model products derived from MERRA-2 offer a reliable source of information for studying various meteorological phenomena related to rainfall. It can be used to investigate changes in precipitation patterns over time, assess the impact of climate change on rainfall distribution and develop predictive models for future weather scenarios. The availability of long-term data also facilitates the study of interannual variability and trends in global precipitation. Overall, the MERRA-2 simulation results based on rainfall data provide an invaluable resource for understanding and predicting precipitation patterns at a global scale. With its extensive time range and accurate assimilation techniques, this dataset is instrumental in advancing our knowledge of Earth's climate system and its complex interactions.

To calculate this factor, the previous formula was applied to 7 MERRA-2 simulation stations located in the Mellegue watershed for the years 2002 and 2018. The precipitation maps are interpolated by kriging using ArcGIS. The produced maps (Fig. 3) show that the highest rainfall is observed in the north of the basin (between 600 and 750 mm/year), unlike the southern regions, which show the lowest rainfall (between 350 and 500 mm/year). Overall observation shows that the P values in 2002 oscillate between 330 and 650 mm/year with $P_{24} = 31.3$ mm, and the annual P values for 2018 vary between 420 and 750 mm with $P_{24} = 37.06$ mm (Table 1).

The calculation of the R factor, which is crucial for assessing soil erosion potential, was carried out using the raster calculator feature within the highly regarded ArcGIS software. This tool empowers users to devise and execute map algebra expressions based on the R factor equation, ensuring that all essential parameters are duly considered. Within the confines of this specific framework, the singular requirement entails having access to the comprehensive rainfall map of the particular catchment region, which serves as the vital input. Notably, this input parameter necessitates the inclusion of two constants that denote the utmost daily precipitation values corresponding to the juxtaposed years of 2002 and 2018. By adhering strictly to these specifications, a more comprehensive understanding can be attained regarding the dynamic fluctuations and trends within the given catchment's precipitation patterns during these specific timeframes. The final outcome of this calculation is a highly informative raster representation depicting the distribution of the R factor across the catchment area. While it is not feasible to utilise the rain erosivity factor for individual stations as an input, it can be interpolated once the R factor map has been generated.

Soil erodibility factor

The soil erodibility factor (K) defines the average loss (in tons/year) per unit area for a particular field assumed to be unplanted (soil type and cover) whose slope has been set by default at 72.6 ft in length and at 9% inclination. This factor exposes the cohesion and resistance of soil particles to detachment and transport by water erosion agents (rain and runoff). It depends mainly on the texture but on other parameters, such as the organic matter content, the structure and the permeability of the soil.

The K factor was calculated using a soil map dispersed throughout the catchment region that was
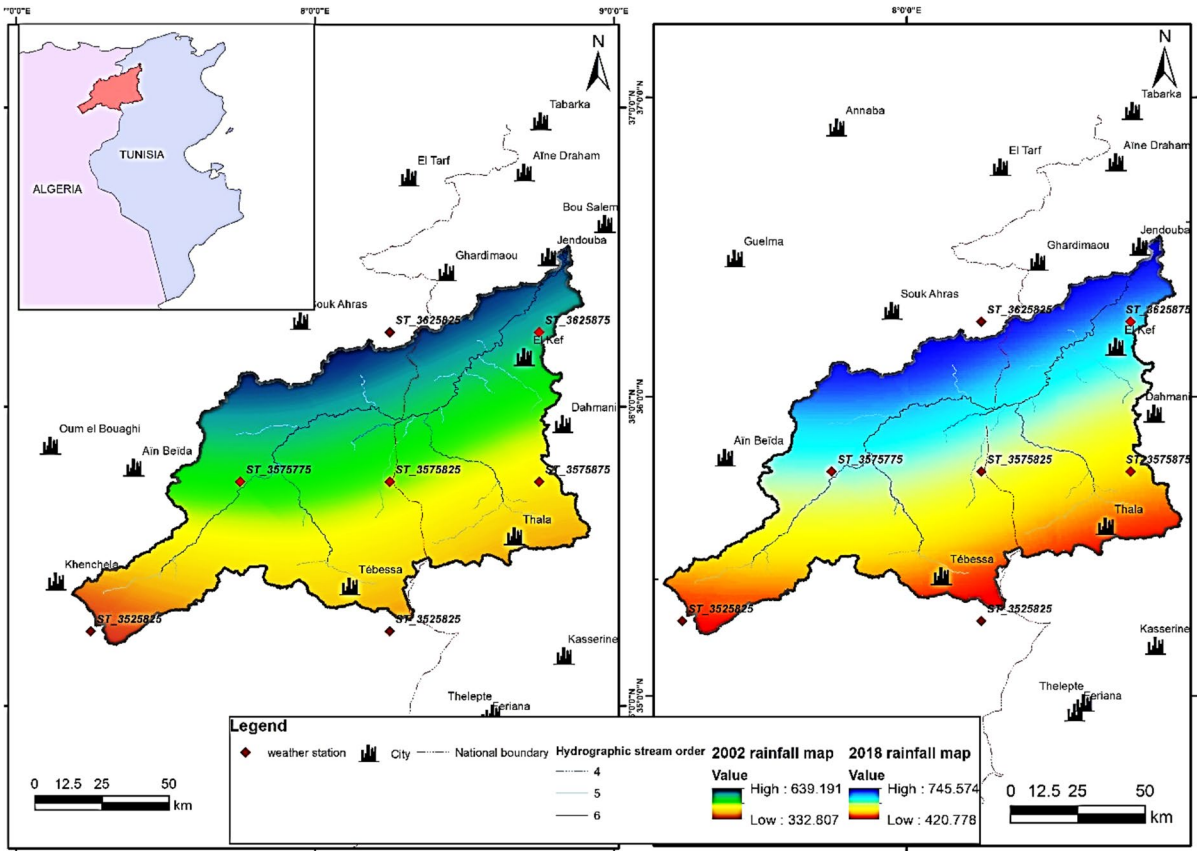
Fig. 3 2002 and 2018 Rainfall maps for the watershed of the Mellegue

Table 1 Coordinates of weather stations within the Mellegue watershed

Merra-2 simulation station	Name	LAT	LON	2002			2018		
				Annual rainfall	Max rainfall (24 h)	Median	Annual rainfall	Max rainfall (24 h)	Median
1	ST_3525725	35.25	7.25	339.22	18.86	31.3	445.3	50.08	37.06
2	ST_3525825	35.25	8.25	396.78	30.88		425.48	26.95	
3	ST_3575775	35.75	7.75	501.76	27.52		598.99	40.13	
4	ST_3775825	35.75	8.25	484.32	34.87		574.88	37.06	
5	ST_3575875	35.75	8.75	651.83	34.82		507.2	29.08	
6	ST_3625825	36.25	8.25	649.06	32.95		738.04	40.7	
7	ST_3625875	36.25	8.75	564.96	31.3		651.38	35.57	

clipped from a digitised version of the FAO-UNE-SCO Soil Map of the World at a scale of 1:5 million (Latham, 1981). It depicts 4931 mapping units made up of soil associations (mixtures of distinct soil types) defined according to the FAO-UNESCO legend, which specifies a total of 106 soil units based on the existence of diagnostic features and 4 non-soil units. The Soil Map of the World (SMW) has been superseded by the Harmonized World Soils Database (HWSD), which offers more extensive information on soil distributions

for a number of nations gathered after the release of all volumes of the Soil Map of the World. Experiments on different types of soils allowed the option to statistically develop a set of dedicated equations for the calculation of this factor (Beretta-Blanco & Carrasco-Letelier, 2017; Martínez-Murillo et al., 2020; Vaezi & Sadeghi, 2011). These advanced calculations are able to reclassify the soil map to attribute the variation of the K factor over the entire catchment area. K values are bounded between 0 and 1, where soils with values that approach 0 are the least susceptible to erosion. The determination of the K factor is based on the method of Anache et al. (2015), which characterises the runoff ability of the soil. The K factor values are shown in the following table (Table 2).

Topographic factor

It translates the characteristic factors of the slope (length and inclination). It corresponds to a ratio of sediment losses (under given conditions) to overall soil losses at a specific location defined by an inclination, assumed by default, of 9% and 72.6 slope length feet.

The LS factor was calculated by ArcGIS based on the digital elevation model (Shuttle Radar Topography Mission (SRTM)). The methodology was applied to each pixel of the SRTM file. The calculation of this factor was based on the equation developed by Mitasova et al. (1996):

$$LS = (1.6) \times \left(\frac{A}{a_0} \right)^{0.6} \times \left(\frac{Sin b}{b_0} \right)^{1.3}$$

Where:

A: upward-sloping drainage surface *expressed in square metres per metre* ($m^2 m^{-1}$); b is the slope *angle expressed in degrees* [°]; a_0 is the standard slope length (default equal to 22.1 m (72.6 ft)); b_0 is the standard slope inclination (by default equal to 0.09 (9% or 5.16°)).

The spatial analysis toolbox of the ArcGIS software was used to conceive raster layers of slope gradient expressed in degrees, and from the hydrology toolbox, the flow direction and the flow accumulation were calculated. The output layers were then used in the software's raster calculator interface to generate the LS factor map based on the following equation using the *flow* accumulation grid:

$$LS = POW \left(\frac{[Flow\ Acc] \times resolution}{22.1}, 0.6 \right)$$
$$\times POW \left(\frac{(\sin [slope\ gradient] \times 0.01745)}{0.09}, 1.3 \right)$$

Where [Flow acc] is the flow accumulation in ArcGIS. It is determined from the flow direction of the raster. The soil is too susceptible to erosion risk when the slope is steeper and/or longer. This is due to the gradual accumulation of runoff in the downward slope. Secondly, the more the slope increases, the more the soil erosion intensifies due to the increase in the speed and erosivity of the runoff.

Vegetation cover factor

The C factor is a generalised value that reflects the type of crop without taking into account any other external factors, such as crop rotations or climate (annual and geographical distribution of precipitation). However, the C factor compares soil losses between the different types of plant cover (dense vegetation, bare soil and soil characterised by specific management). The values of C vary between 0.001 (dense forest) and 1 (bare soils). Many methods exist for the computation of this factor (Almagro et al., 2019; Yan et al., 2020; Zhao et al., 2012). Among these methods, remote sensing data offers the possibility of calculating the vegetation cover factor. The most common method is based on the Normalised Vegetation Index (NDVI), which provides

Table 2 Assignment of K factor according to soil type	Description	Soil code (FAO)	Sand (%)	Silt (%)	Clay (%)	Organic carbon (%)	K factor
	Calcic Cambisols	**BK**	81.6	6.8	11.7	0.44	0.014
	Calcareous Fluvisols	**JC**	39.6	39.9	20.6	0.65	0.023
	Haplic Xerosols	**XH**	54.8	20.6	24.9	0.53	0.020
	Calcic Xerosols	**XK**	48.7	29.9	21.6	0.64	0.022

information on the type and health of the vegetation cover (Durigon et al., 2014; Karaburun, 2010; Rawat & Singh, 2018). The C factor is calculated according to the following formula (van der Knijff et al., 2000):

$$C = \exp\left[-\left(\frac{\alpha \text{NDVI}}{\beta - \text{NDVI}}\right)\right]$$

Where α and β represent deterministic factors of the curve trend which joins the NDVI to factor C. However, the authors attribute, by default, to α and β the values of 2 and 1, respectively. NDVI is a plant health indicator that assesses a plant's ability to reflect light at specific frequencies (some waves are reflected, others are absorbed). Visible light is strongly absorbed by chlorophyll, which is a health indicator. On the other hand, leaves strongly reflect near-infrared due to their cellular shape. The spongy layer becomes less effective when the plant is dry or ill, which causes it to absorb more near-infrared light rather than reflecting it. Thus, the existence of chlorophyll, which is associated with plant health, may be accurately detected by measuring how near-infrared (NIR) changes in comparison to red light. As a result, the NIR and red waves are used to calculate NDVI using the following equation:

$$\text{NDVI} = \frac{\text{NIR} - \text{RED}}{\text{NIR} + \text{RED}}$$

The vegetation density (NDVI) at a certain coordinate of the picture is the intensity difference of the reflected lights in the red and near-infrared divided by the total of these intensities, according to this formula. This index has a value range of -1 to 1, signifying mainly vegetation, with negative values referring to unvegetated places (clouds, water and snow) and average values of zero defining bare ground. Shrubs and grasses have moderate values (0.2 to 0.3), whereas dense vegetation has high values (0.6 to 0.8). This NDVI interval is effectively used in crop monitoring to indicate to users whether areas have thick, moderate or sparse vegetation at any particular moment.

Accordingly, the measurement of the NDVI utilised data obtained from multispectral satellite imagery captured by Landsat 7 (ETM+) and Landsat 8 (OLI) for 2002 and 2018, respectively. By accessing these high-resolution images, the researchers were able to precisely assess the level of vegetation vigour and vitality based on the varying reflectance of different light wavelengths. The use of satellite imagery facilitated a comprehensive analysis of changes occurring in vegetation over the time period, enabling deeper insights into the alterations and fluctuations in the ecological landscape. With this objective information, a clearer understanding of the evolving vegetation patterns and potential environmental impacts can be attained.

Anti-erosion practices factor

It corresponds to the conservation practice factor. It reflects the impacts of cultural practices on the magnitude of erosion risk. This factor represents the ratio of land loss relative to a given conservation practice to land loss associated with row cropping within the same slope direction. The P factor was calculated according to Shin (1999), whose values depend on the slope, according to the following table (Table 3):

Results and discussion

The RUSLE model, a widely utilised approach in soil erosion assessment, was elegantly employed to accurately quantify soil losses within the Mellegue watershed. To obtain comprehensive insights, each of the model's distinct factors, such as rainfall erosivity, soil erodibility, slope length, slope steepness and crop management, were meticulously calculated and spatialised in a GIS environment. By considering and analysing these various parameters, we can effectively establish and delineate the extent of erosion loss that occurred between 2002 and 2018 across the entirety of the given basin. This comprehensive evaluation enables us to accurately quantify and map the erosion patterns, providing valuable insights into the changes that have taken place over time.

Table 3 Assignment of P factor in terms of slope (Shin, 1999)

Slope (%)	P factor
[0–7]	0.55
[7–11.3]	0.60
[11.3–17.6]	0.80
[17.6–26.8]	0.95
>26.8	1.00

This enabled a sophisticated integration of spatial data, promoting a holistic understanding of the intricate interplay between environmental variables. Such an analytical framework aids in formulating sustainable soil conservation strategies, mitigating erosion's adverse impacts and safeguarding the long-term productivity of the watershed for the benefit of all stakeholders.
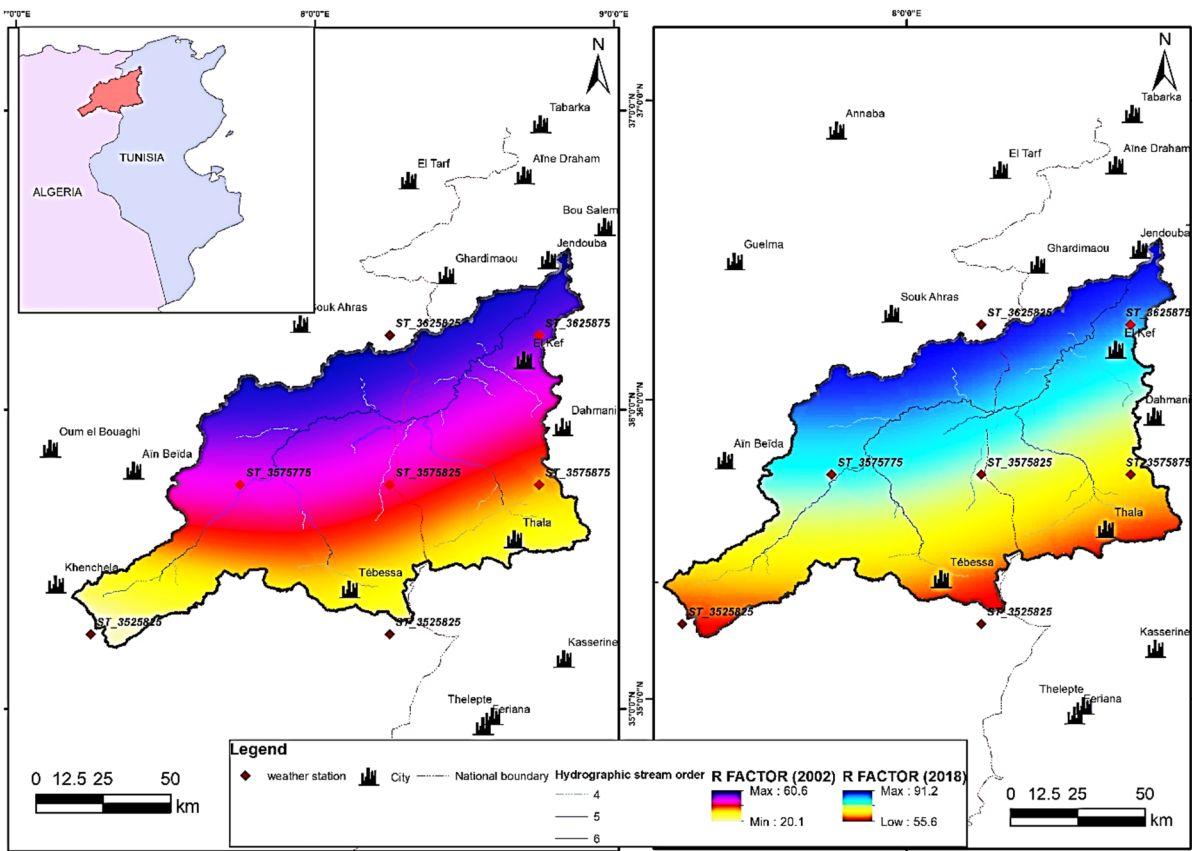
Rain erosivity factor

The erosivity of rainfall in the Mellegue watershed varies between 20 and 60 MJ mm/ha/h/year in 2002 while it fluctuates between 55 and 91 MJ mm/ha/h/year in 2018 (Fig. 4). The average values deduced from the R factor in 2018 (75 MJ mm/ha/h/year) are higher than those of 2002 (44 MJ mm/ha/h/year). The general pattern of rainfall aggressiveness within the basin shows an increasing gradient from *south to north*. Consequently, the values of R show

that the basin is subjected to a high pluvial aggressiveness, which reflects a significant erosive power of precipitation on the basin. Regardless of the year, the spatial distribution of R values shows that 30% of the area of the basin (generally located in the north) is exposed to intense erosive power from rainfall.

Soil erodibility factor

The K factor calculated in the Mellegue watershed varies from less than 0.014 to 0.023 t/h/ha/MJ/mm, with an average equal to 0.018 t/h/ha/MJ/mm, which is relatively low (Fig. 5). The lowest values are mainly located in the *centre* of the basin, where the soils are calcareous and moderately rich in organic matter, providing high penetration rates and limiting runoff. In addition, the area is further protected by vegetation, where grasslands, shrubs and sparse forest

Fig. 4 2002 and 2018 erosivity factor (R) for the Mellegue watershed

are the dominant vegetation cover. The high values are located in the marl-clay soils, covering 49.5% of the basin's total area.

Topographic factor

In the Mellegue catchment, LS values vary from 0 to 525 and have been grouped into five classes (Fig. 6; Table 4). The results obtained depend on the length and degree of the slope inclination. Overall analysis shows that the average value of LS is equal to 1.9, where the class [0–2] occupies 70% of the basin area (Table 4). This corresponds to areas of low altitude and plains. A high LS index (greater than 30) represents only 3% of the area of the basin. The spatial dispersion of this factor also shows that the very high values are located in the intrusive zones of the tributaries. These areas bear witness to the most sensitive regions to erosion. Nevertheless, it has been reported that the risk of erosion increases exponentially (with an average exponent of 1.4) depending on the degree of slope (Elbouqdaoui et al., 2005). Similarly, it has been shown that the kinetic energy created by precipitation becomes constant in favour of a slope with a high degree of inclination. In contrast, the velocity of the sediment transport process rises downward due to the increase in kinetic energy created by runoff (Nord, 2006).

Vegetation cover factor

The C factor reflects the cover and degree of crop production. For 2002 and 2018, maps of the spatial distribution of the C index show that low vegetation density classes are mostly vulnerable to erosion (Fig. 7).

The results obtained from the C factor map in 2002 confirm that 77% of the area of the basin shows a very low vegetation rate (C factor > 0.5), and only 23% of the area is well protected with a C
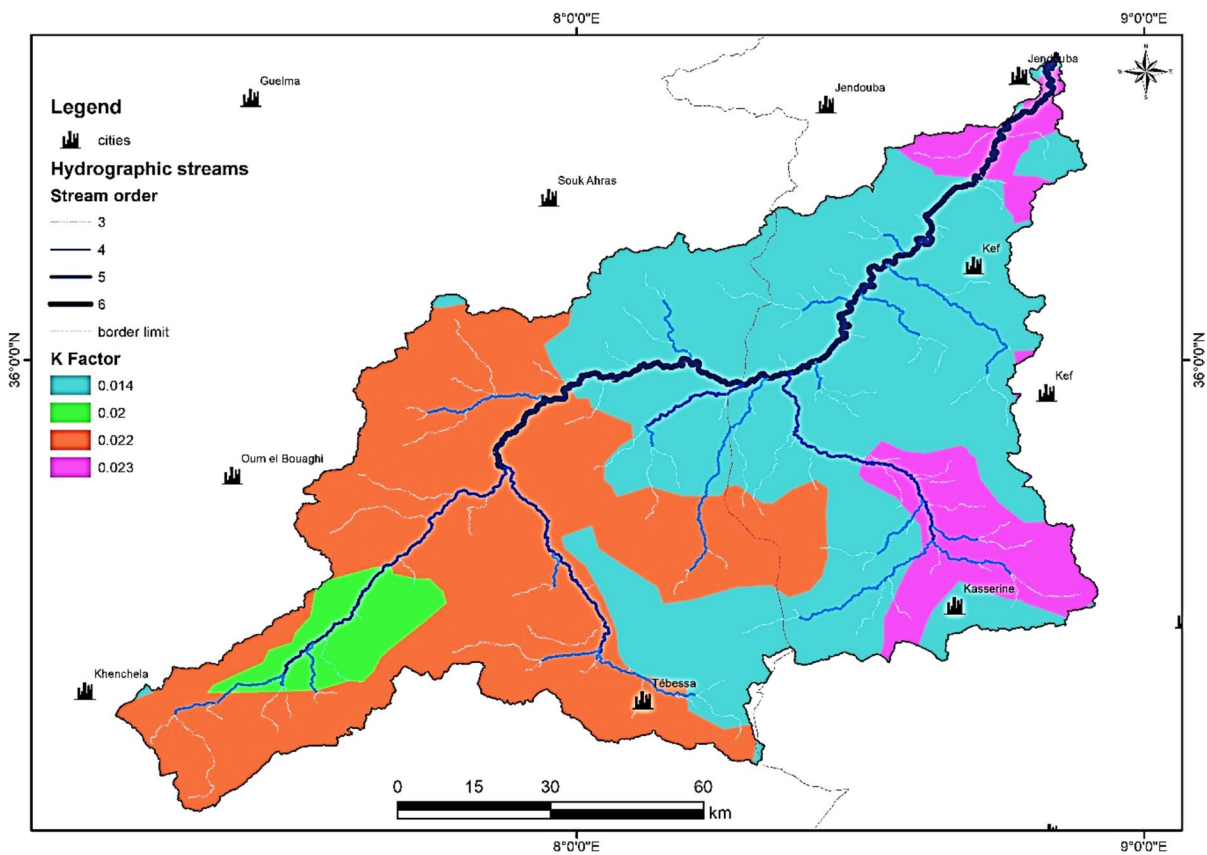
Fig. 5 Erodibility factor (K) map of the Mellegue watershed
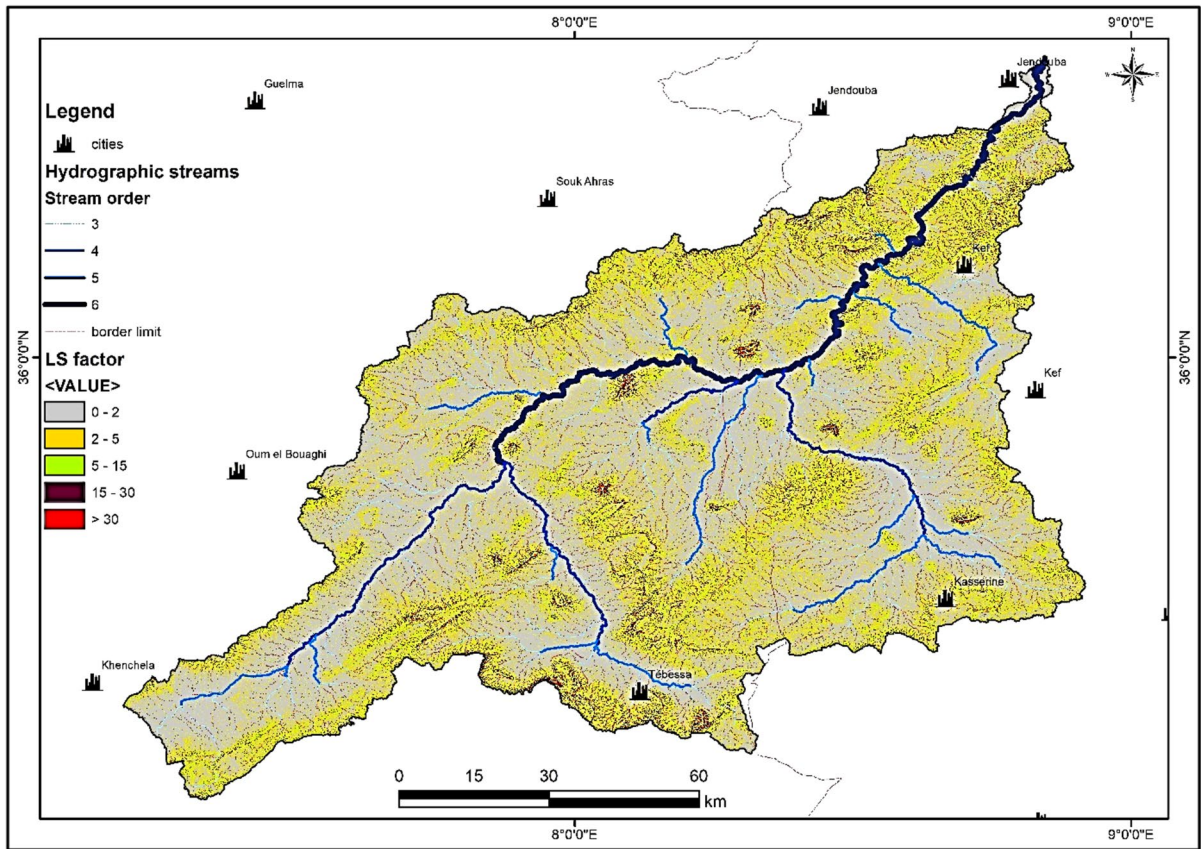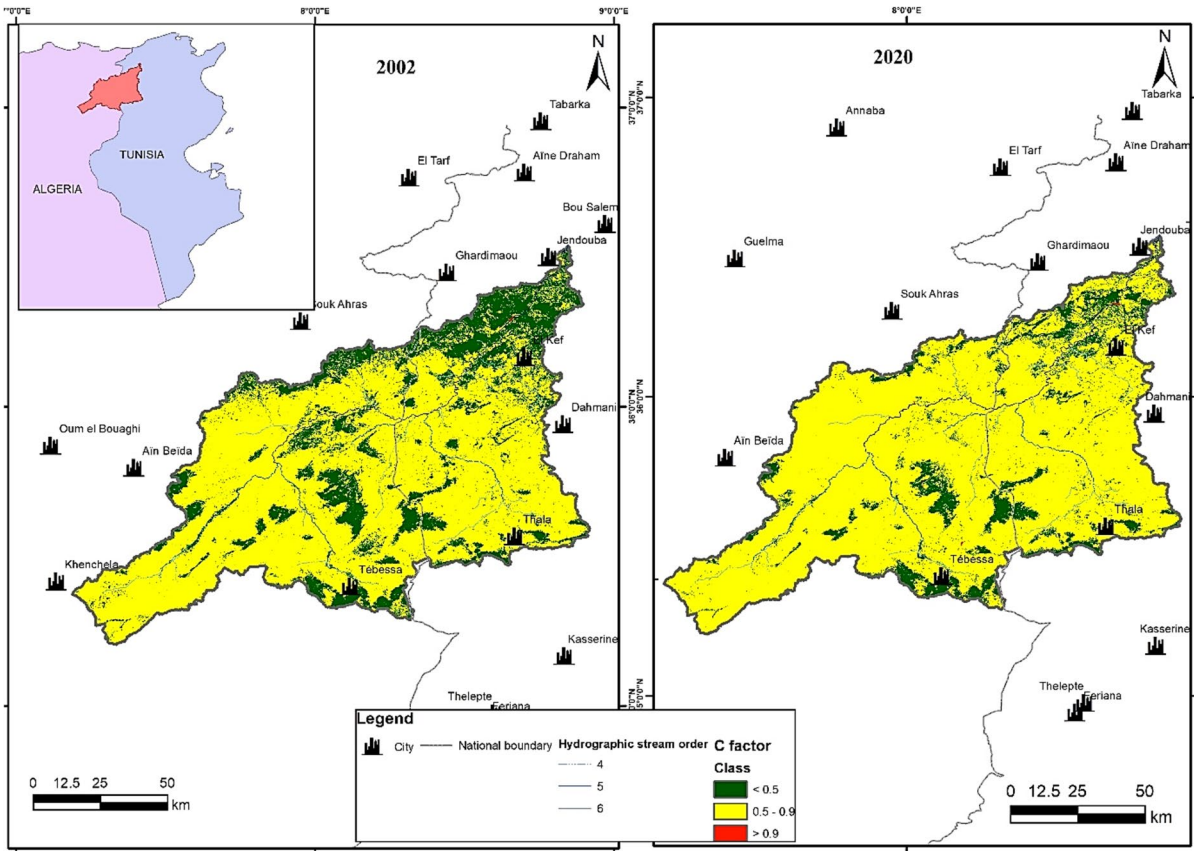
Fig. 6 LS factor map of the Mellegue catchment

Table 4 Occupancy rate (in km² and %) of the LS factor classes within the catchment of the Mellegue

LS factor class	Area (km²)	Occupancy rate (%)
[0–2]	7340	70
[2–5]	1349	13
[5–15]	1199	11
[15–30]	353	3
> 30	303	3
Sum	10,544	100

factor < 0.5. This protected area was reduced in 2018 to only 13% of the total area of the basin (C < 0.5). The low vegetation cover reflects open forests, cultivated land, degraded rangelands and sylvatic areas, which are generally very sensitive to erosion. Values below 0.5 are related to dense vegetation such as forests, matorrals and arboriculture, while values between 0.5 and 0.9 relate to moderately covered vegetation such as open matorrals and sparse forests. The extreme values of the C factor, which tend toward, 1 relate to bare soils and harvested field crops.

The analysis of the spatial distribution of the C factor in 2018, compared to 2002, confirms that sensitive areas to water erosion (with a C factor > 0.5) have been well developed, especially downstream of the catchment. The increase in low vegetation cover areas (C factor > 0.5) has been intensified by the conversion to land that favours water erosion, such as cultivated land and steppes. The spatial distribution of the C factor confirms that the study area experienced a degradation of dense vegetation following the sociopolitical events that occurred in Tunisia in 2011, manifested in the form of anthropogenic actions and anarchic land conversion that have severely impacted forests and vegetation in the region (Chriha & Sghari, 2013).

Fig. 7 2002 and 2018 vegetation cover (C) factor maps for the Mellegue catchment

Anti-erosion practices factor

Cultivation techniques commonly used, such as cultivation following the contour lines direction, ridging, terracing or alternating strips and ridging are effective practices for soil conservation against erosion. The values of the P factor depend on erosion control, the agricultural practice carried out and also on the slope.

In this study, *P* values were concluded on the basis of slope. Low and medium values correspond to areas with low to moderate slopes. The spatial distribution of the P factor within the catchment area shows that values between 0.55 and 0.6 (areas with low slope) occupy 76% of the catchment area, while values between 0. 6 and 0.8 (zones with moderate slope) represent 11.9% of the area. The steeply sloping areas (*P* between 0.8 and 0.95) define 7.1% of the basin area. Finally, the values that tend toward the external higher limit (equal to 1) and that correspond to land

without anti-erosion practices constitute 5% of the study area (Fig. 8).

Soil loss assessment

The estimated soil losses were obtained by combining the factors of the RUSLE model, which are soil erodibility (K), climatic aggressiveness (R), vegetation cover (C), topographic factor (LS) and anti-erosion practices (P). The combination of these factors in a GIS environment provides accurate maps of soil losses, which we can observe the spatial distribution of this phenomenon throughout the entire catchment area.

Soil losses in the Mellegue watershed were estimated at 25,584 t/year for 2002 with an average of 1.58 t/ha/year and a standard deviation of 52 t/ha/year, against a total loss estimated at 53,822 t/year in 2018 with an average of 1.78 t/ha/year and a standard deviation of 66 t/ha/year. This states the importance

and great variability of the water erosion phenomenon, which has intensified considerably in 2018 compared to 2002. Soil losses have been grouped into 5 classes (Figs. 9 and 10; Tables 5 and 6). The first class concerns areas where soil loss is less than 7 t/ha/year. It represented 94.9% of the area of the basin in 2002 and 91.7% in 2018. This class mainly dominates where it is seen throughout the basin. The second class concerns areas where soil loss is between 7 and 15 t/ha/year. It occupied 2.1% in 2002 and 3.8% in 2018 of the basin's total area. The third class represents areas of soil loss estimated between 15 and 30 t/ha/year. This class constituted 0.9% (90 km^2) in 2002 and 1.7% (181 km^2) of the total area of the basin in 2018. The fourth class contains areas whose soil loss is between 30 and 60 t/ha/year. The occupations of this class are very low since they represented only 0.3% (31 km^2) of the total area of the basin in 2002 against 0.8% (85 km^2) in 2018. In regard to the unclassified category, the model faced difficulty in

detecting all the essential factors (C, R, K, LS and P) within certain pixels to accurately calculate the extent of soil loss. It is crucial to emphasise that these unclassified spots, accounting for only 1% of the overall catchment area, are a common occurrence. Despite their frequency, it is important to acknowledge that more comprehensive data are required to effectively assess and address soil erosion in those areas. The last class concerns losses in upper soils at 60 t/ha/year. It bears witness to the mountainous areas as well as the areas with friable substrate located on either side of the basin. This class represented 0.3% (33 km^2) of the total area in 2002, against 0.5% (57 km^2) in 2018. The steep slopes and marly–clayey soils of the hills play host to maximum soil loss. The mountainous regions and the areas with friable substrates located on both sides of the basin also contribute to high soil erosion. The identification of the friable substrate was accomplished through extensive field surveys, as it could not be discerned on the K map due to its interpolation
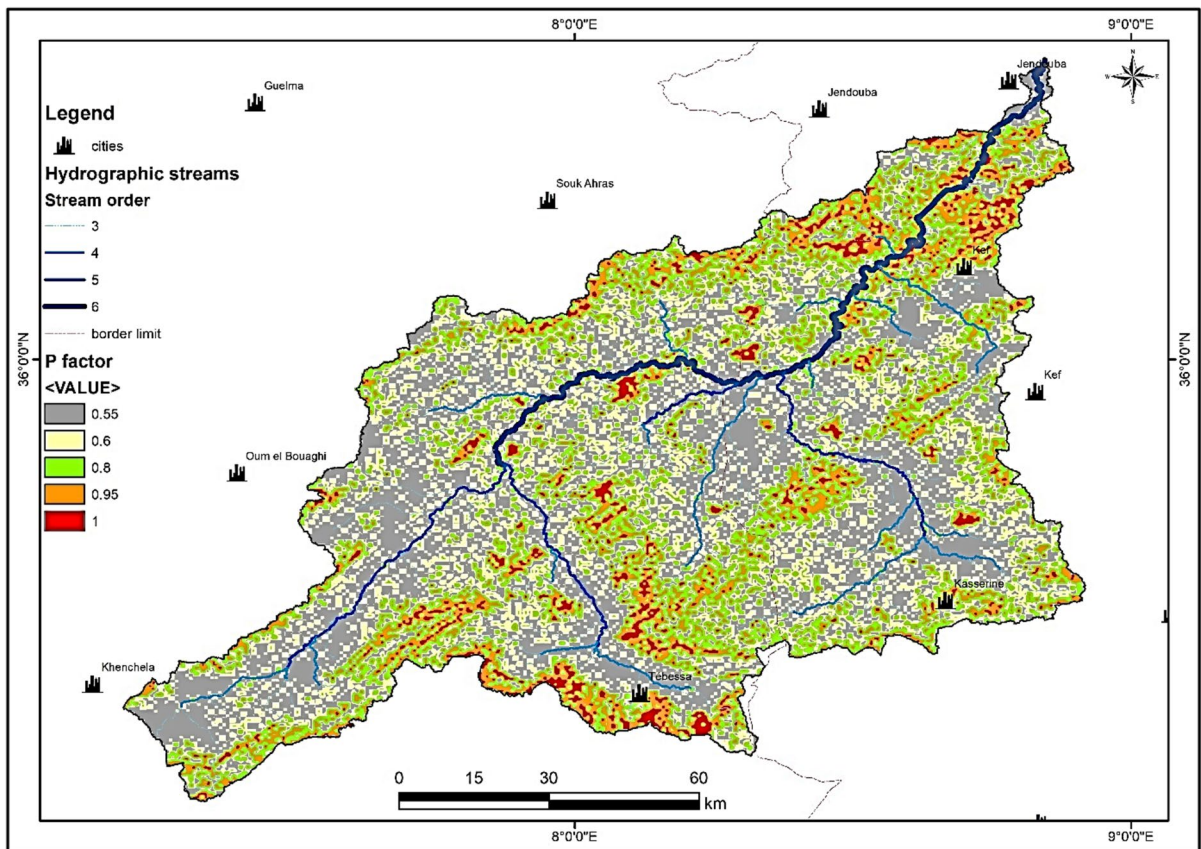
Fig. 8 P factor map for the Mellegue catchment
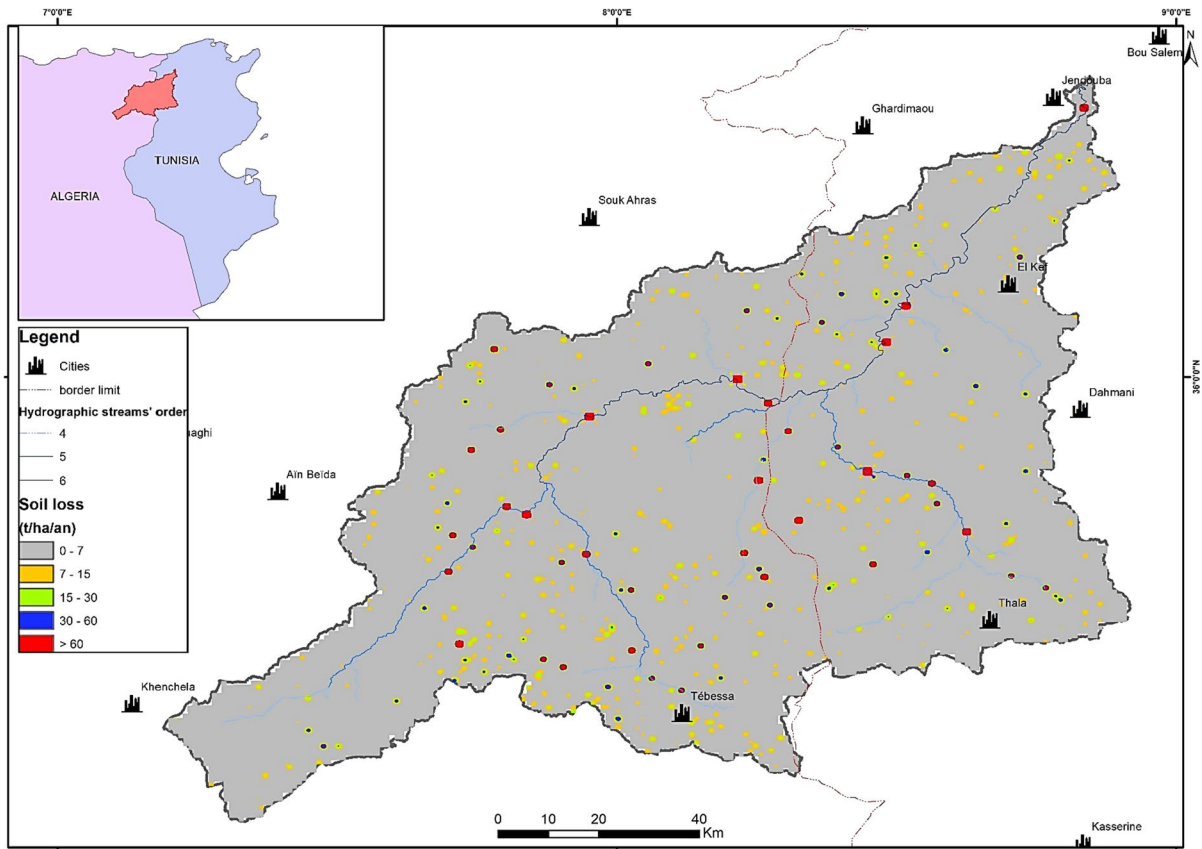
Fig. 9 2002 soil loss map of the Mellegue catchment

based on the general scale of the FAO soil map. By incorporating the findings from these studies, we gain a deeper understanding of the factors contributing to soil loss in the region.

The identification of the friable substrate was meticulously conducted through local, rigorous field survey studies, ensuring a high level of accuracy and reliability. This crucial determination, however, could not be ascertained by solely relying on the K map. The reason lies in the fact that the K map is constructed through interpolation, using the general scale of the FAO soil map. Field survey studies serve as essential tools in the assessment and classification of substrates, as they involve detailed observations and measurements taken at specific locations of interest. These studies encompass a wide range of methods, including on-site sampling, laboratory analysis and examination of physical and chemical properties of the substrates under investigation. The information obtained through such meticulous fieldwork is pivotal

in understanding the nature and characteristics of the friable substrate.

In contrast, the K map, which is constructed based on the general scale of the FAO soil map, provides valuable insights into the broader soil composition and distribution patterns. It offers a valuable overview but lacks the specificity and granularity needed to identify the friable substrate accurately. The interpolation technique used in generating the K map focuses on estimating values for areas where data points are limited, potentially leading to inconsistencies when it comes to identifying the friable substrate.

Therefore, due to the inherent limitations of relying exclusively on the K map, the identification of the friable substrate necessitated field survey studies. These comprehensive investigations allowed for meticulous observations and analysis, enabling a precise determination of the friable substrate's characteristics, distribution patterns and physical properties. This approach ensures the integrity and
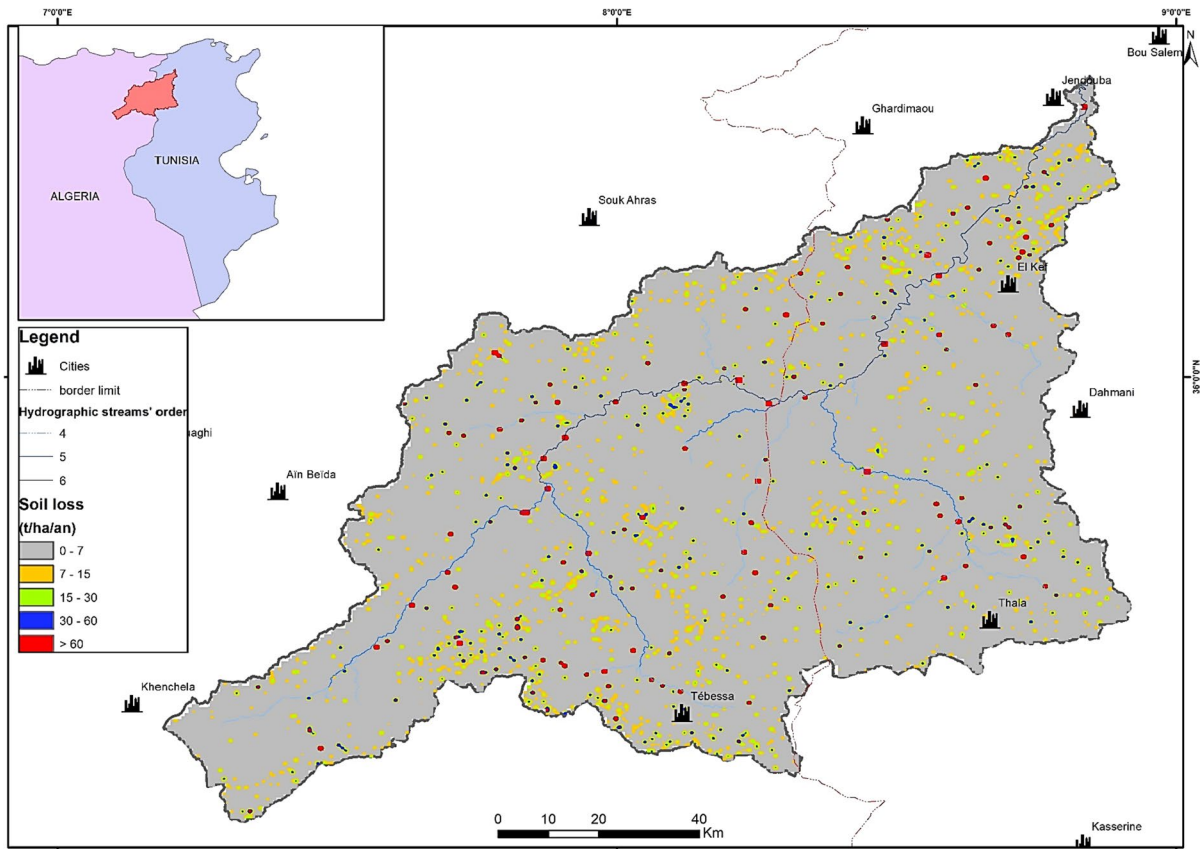
Fig. 10 2018 soil loss map of the Mellegue catchment

reliability of the findings, avoiding any inaccuracies or misinterpretations that could arise from relying solely on map data.

Thus, in-depth analysis shows that the areas with a high erosion rate (greater than 30 t/ha/year) evolved from 64 km^2 (i.e. 0.6% of the total area) in 2002 to 142 km^2 (i.e. 1.3% of the total area) in 2018. This figure reflects a non-compensable soil loss, mainly by the effect of pedogenesis. The results show a reduction in areas with a low risk of erosion (between 0 and 7 t/ha/year) against an increase in all the other classes. This confirms the degradation of soils and the intensification of the phenomenon of erosion in the Mellegue watershed.

These results obtained, either for 2002 or 2018, are very close to the other studies that were established under similar conditions and applied only upstream of the Mellegue watershed, where low soil loss areas represent 80% of the area of the basin (Khanchoul et al., 2020). In addition, the reported results are close

to several other studies whose methodology is based on RUSLE modelling, where climatic and spatial characteristics are similar to those of the Mellegue catchment (Goumrasa et al., 2021; Khemiri & Jebari, 2021; Mahleb et al., 2022; Serbaji et al., 2023).

Minimal soil loss occupies most of the watershed. It is the result of the action of land with a low slope, generally less than 3%. This is also explained by the low values of the LS factor and, above all, by the protective effect of vegetation in sloping areas. On the other hand, values of soil losses greater than 30 t/ha/year (64 km^2 in 2002 and 142 km^2 in 2018) are mainly located in areas with steep slopes where the soil is fragile and composed of marl and clay. This area is characterised by high to very high erosion intensity. The variation in soil losses shows that it is greater downstream than upstream of the basin. The phenomenon intensified further in 2018. Estimated soil losses in the Algerian part of the basin increased from 14,265 t/year (i.e. 56% of the total loss) in 2002

Table 5 Comparative soil loss rates in the Mellegue watershed between 2002 and 2018

Class (t/ha/an)	Erosion rate	2002						2018					
		Tunisia		Algeria		Sum		Tunisia		Algeria		Sum	
		Area (km^2)	Area (%)	Area (km^2)	Area (%)	Area (km^2)	Area (%)	Area (km^2)	Area (%)	Area (km^2)	Area (%)	Area (km^2)	Area (%)
Unclassified	–	70	1.6	87	1.4	157	1.5	72	1.6	80	1.3	152	1.4
0–7	Very weak	4173	94.9	5837	95.0	10,010	94.9	4036	91.7	5633	91.7	9669	91.7
7–15	Weak	96	2.2	127	2.1	223	2.1	162	3.7	239	3.9	400	3.8
15–30	Moderate	32	0.7	58	0.9	90	0.9	74	1.7	108	1.8	181	1.7
30–60	High	15	0.3	16	0.3	31	0.3	34	0.8	51	0.8	85	0.8
>60	Very high	12	0.3	21	0.3	33	0.3	22	0.5	35	0.6	57	0.5
Total	–	4399	100	6145	100	10,545	100	4399	100	6145	100	10,545	100

to 30,603 t/year (i.e. 57% of the total loss) in 2018 (Table 6). By analogy, the sediment loss from the Tunisian part of the basin has also evolved, starting from 11,319 t/year in 2002 to 23,219 t/year in 2018. Although the Tunisian area belonging to the basin constitutes 40% of the area, it seems that the estimated soil losses of this part are close to the sediment losses from the Algerian territory of the basin. However, the spatial–temporal comparative tools of GIS, carried out on the maps of 2002 and 2018, show the appearance of 13,954 new areas at risk of water erosion in 2018 compared to 2002. Almost 60% of these areas are observed in Algerian territory, while the rest are in Tunisia.

Sediments extracted from upstream are likely to settle downstream rather than being transported out of the basin. In addition, the local sedimentation that took place in the flow axes and the superficial depressions will contribute to the filling of the watercourses, and drainage problems may appear (Mounirou, 2012). This phenomenon promotes slope instability, gully erosion and landslides. Anthropogenic action influences the intensity of water erosion. The intensification of agricultural land use observed within the watershed during the period from 2002 to 2018 has contributed to accelerating water erosion. Several causes are involved, such as the choice of cropping systems and the excessive exploitation of land, as well as the application of unsuitable agricultural techniques, namely: too frequent ploughing and following the slope direction, overgrazing and poor management of irrigation (Braiki, 2018).

Many causes can lead to the intensification of soil loss. The area has witnessed urban extension taking place during the period (2002–2018) which took place rapidly at the expense of several classes of land use, in particular forest cover (Weslati et al., 2023). The artificial soils of the urban environment will prevent the infiltration of rainwater, and therefore the volumes of water to be evacuated will be enormous. This process increases soil erosion, which generates different patterns of degradation. The reduction of forest space in the region has increased the process of erosion, causing floods and mudslides. The outlet of the watershed forming part of the Jendouba region constitutes a favourable environment for water erosion (Fehri, 2014). In addition, the region has been marked by repetitive historic floods, causing material and human damage (Sahar et al., 2019). Maps dating

Table 6 Comparative average soil losses in the Mellegue watershed between 2002 and 2018

	2002			2018		
	Tunisia	Algeria	Total	Tunisia	Algeria	Total
Number of risk areas	6775	9487	16,262	12,583	17,633	30,216
Total soil loss (t/an)	11,319	14,265	25,584	23,219	30,603	53,822
Average (t/ha/an)	1.67	1.50	1.58	1.85	1.74	1.78
Standard deviation (t/ha/an)	50	15.8	52	59	65.25	66

from 2002 and 2018 show a high rate of mobilised sediment in this region exceeding 1000 t/ha/year.

The relationship between rainfall erosivity and erosion potential becomes evident when examining the modelling of rainfall patterns. Figure 4 aptly illustrates that rainstorms that are both stronger and longer in duration possess a higher capacity for causing erosion. Furthermore, the LS factor map reveals a significant correlation between the length and steepness of a slope and the amount of runoff it generates over an extended period of time. As the slope becomes steeper, the velocity of the runoff increases, leading to a greater likelihood of erosion. This observation was likewise supported by the research of Wischmeier & Smith (1958). Furthermore, in the Mellegue watershed, a fascinating exploration into hydrological patterns has unravelled the existence of five distinct seasons. These seasons not only witness variations in rainfall but also experience fluctuations in the transport of solid and/or liquid materials, consequently affecting the erosivity factor. This intriguing finding highlights the complexity of erosion dynamics within the Mellegue watershed.

In addition, their findings also emphasise the impact of plant cover on erosion control. Extensive research reveals a crucial relationship between plant cover and erosion, as it has been discovered that plant cover plays a vital role in mitigating the erosive forces induced by rainfall. By skillfully intercepting rainwater, plant cover effectively reduces its energy, allowing for enhanced rainfall penetration. Accordingly, the correlation between land use and land cover changes and soil loss cannot be understated. In order to accurately determine the impact of these changes, it becomes necessary to assign C-factor values to the various land cover classes within the study area. However, achieving this level of precision demands a comprehensive understanding of the area's cover characteristics, including the ability to map and monitor them accurately. While this method may be

suitable for smaller scales such as fields or farms, the sheer size of a watershed makes it impractical to monitor all these characteristics feasibly. Consequently, alternative approaches must be considered when assessing soil loss on a watershed scale.

In conclusion, when it comes to determining C factors for small-scale studies, conducting fieldwork is often the most feasible approach. However, if previous studies using the RUSLE have reported C factors for a cover similar to the study area, it may be appropriate to use those values through a table-based approach. Additionally, high-resolution imagery can be utilised to determine the NDVI for the study area. At small scales, where there is a good understanding of the differences in land cover classifications, pulling values from existing literature may be the most efficient choice. However, this may become tedious at larger regional scales. In these cases, high-resolution satellite imagery may be available to determine NDVI. It is important for authors to be mindful of the acquisition date of the imagery in relation to their study period. Furthermore, pre-processing steps such as masking cloud cover and creating aggregates from these masked images are necessary (Kulikov et al., 2016; van der Knijff et al., 2000).

The effectiveness of a conservation practice in mitigating soil erosion is directly correlated to the P factor, as stated by Bagherzadeh (2014). Similar to the C factor, literature can provide values for the P factors. In cases where no support practices are observed, the P factor is assigned a value of 1.0 (Adornado et al., 2009). Alternatively, subfactors can be used to estimate the P factor. However, accurately mapping support practice factors or not observing support practices often leads to studies disregarding the P factor and assigning it a value of 1.0 (Adornado et al., 2009; Renard et al., 1976; Schmitt, 2009). One possible reason for studies neglecting the P factor is that some chosen C factors already account for the presence of support factors like intercropping or contouring. For

instance, Morgan (2005) and David (1988) provide C factors specific to one crop but with different management techniques employed.

In spite of its often overlooked importance, numerous studies have identified potential P factors for various types of agricultural practices, including tillage, terracing, contouring and strip-cropping. By incorporating these P factors at detailed scales and with a good understanding of farming techniques, we can achieve more accurate estimations of soil loss. Additionally, these P factors can be utilised in scenario analysis to assess how changes in agricultural practices may mitigate or worsen soil erosion. It is worth noting that the P factor can significantly impact the estimated soil loss, such as zoned tillage thus reducing soil erosion estimates (Benavidez et al., 2018).

By utilising a combination of field survey studies and the interpretive power of maps like the K map, a more complete understanding of the friable substrate can be achieved. This multifaceted approach is crucial in accurately identifying and assessing the properties of the substrate, contributing to effective land management strategies, environmental planning and sustainable development practices.

The integration of the RUSLE model into the GIS environment ensured efficient management of the large volume of data relating to the various factors of water erosion. It is also possible to generate a synthetic map of the possible erosion rates, expressed in tonnes of sediment lost per hectare per year. This map offers to visualise spatially the distribution of the vulnerability to erosion through the entire area of the Mellegue watershed. However, it should be pointed out that the universal equation of the RUSLE model only makes it possible to evaluate soil losses caused by sheet erosion. The model was based on data applied to small areas, which poses problems of uncertainty when used on a large scale and under different conditions than those where the model was initially adopted. Thus, despite the fact that the reliability of the results obtained is subject to discussion, they can nevertheless guide decision-makers in planning the necessary measures to combat erosion in areas where the risk of erosion is preponderant.

Finally, it should be noted that the application of the empirical RUSLE model under conditions different from those in which it was developed exposes it to numerous errors and criticisms, which will lead to a suspect and irrelevant estimate of soil losses.

Moreover, the model is considered applicable if all these factors are non-zero and do not highlight the deposits. However, the uncertainty is always tolerable, and the results will be more reliable if the field measurements as well as the laboratory analyses are rigorously carried out (Renard et al., 1976).

To determine the accuracy and reliability of the Rusle model, the siltation rate of the Mellegue data can be utilised. Situated approximately 50 km from the outlet, the dam downstream of the watershed serves as a point of reference. However, it is important to note that the sedimentation measurement campaigns conducted between 1975 and 2000 may not provide current and comparable results to recent studies, including this one (Mammou & Louati, 2007). Moreover, the dam has almost reached its silt capacity, rendering further siltation rate measurements obsolete (Cherni et al., 2010; Mammou & Louati, 2007). Thus, it is crucial to consider the most recent siltation values for an accurate analysis. Furthermore, the latest measurement of siltation within the watershed reveals a significant degree of sediment accumulation, approximately 3.89 million cubic metres per year. In a study conducted by Cherni et al. (2010), it was discovered that the transport of solids in the main stream is highly unstable and relies heavily on the seasonal characteristics of the surrounding areas, which have been identified as having five distinct hydrological seasons. On average, the solid transport within the watershed remains relatively low, with an estimated volume of 4.8 million cubic metres annually in the year 2010. These findings highlight the intricate dynamics of sediment movement within this particular ecosystem.

To assess the validity of the RUSLE model when it comes to predicting siltation or solid inputs originating from river systems, it is imperative to consider a comprehensive range of accurate and diverse parameters. These parameters should specifically focus on the maximum and average flows occurring on a daily scale, as they play a fundamental role in determining the magnitude and frequency of sediment transport.

In order to develop a robust understanding of the RUSLE model's performance, it is crucial to gather data on peak flows as well as average flows. Peak flows refer to the maximum volume of water passing through a river channel at any given point in time, while average flows consider the sustained volume of water passing through the river on a daily basis. By

incorporating data on both peak and average flows, a more comprehensive assessment of the model's validity can be obtained.

One of the primary challenges in assessing the RUSLE model's validity lies in obtaining accurate and reliable measurements of these flow parameters. To achieve this, advanced monitoring techniques such as automated gauging stations, remote sensing and numerical simulations can be utilised. These techniques provide real-time data and enable the measurement of flows at specific locations along the river, facilitating a more precise estimation of sediment transport.

Furthermore, it is essential to ensure that the parameters used in the RUSLE model, such as maximum and average flows, are representative of the specific river system under scrutiny. Different rivers have unique hydrological characteristics influenced by factors such as climatic conditions, topography, land use patterns and human interventions. Thus, it is necessary to calibrate the flow parameters based on local conditions to enhance the model's accuracy and applicability.

Additionally, the duration over which the data is collected should be considered. Daily scale data is required since sediment transport processes undergo significant variations within shorter timeframes. By analysing the model's performance at such a fine temporal resolution, potential shortcomings and limitations that might arise due to temporal variability can be identified and addressed more effectively.

To ensure the assessment of the RUSLE model's validity is comprehensive and scientifically sound, it is vital to engage in thorough research and analysis. Proper statistical techniques should be employed to analyse the relationship between the measured flow parameters and sediment inputs. This analysis will help establish the accuracy of the RUSLE model and its ability to predict the siltation or solid inputs originating from the river.

Furthermore, incorporating a range of case studies from different river systems can enhance the generalisability of the findings and increase confidence in the model's validity. By examining how the RUSLE model performs across diverse geographies, it is possible to identify any regional variations or specific factors that may affect its predictive capacity. This information will ultimately contribute to refining the model and improving its applicability in various contexts.

In conclusion, assessing the validity of the RUSLE model in predicting siltation or solid inputs from river systems necessitates careful consideration of numerous parameters, especially maximum and average flows at a daily scale. The accurate measurement of these parameters, along with proper calibration and utilisation of advanced monitoring techniques, will enhance the model's accuracy and applicability. By conducting comprehensive research and analysis, incorporating case studies and utilising statistical techniques, a better understanding of the model's performance can be achieved, facilitating its use in a wide range of scenarios.

Advantages and limitations of RUSLE

The RUSLE models, while widely recognised for their usefulness in predicting soil erosion on agricultural land within the United States, have faced criticism for their limited applicability outside the country. Originally developed based on extensive soil erosion research conducted specifically in the USA, these models may yield inaccurate results when applied to different temperature regimes and land cover scenarios. One particular area of concern lies in the equation used to determine soil erodibility, which has demonstrated reduced accuracy when applied to non-US locations. As a result, caution must be exercised when utilising the RUSLE models in international contexts to prevent potential over- or underpredictions of actual soil loss over a 5-year period (Kinnell, 2010).

RUSLE enhancement was proven to be effective at modelling erosion in changing circumstances (Wischmeier & Smith, 1958). In terms of making the best use of the database, RUSLE has an edge over USLE since it combines empirical and process-based design. RUSLE components are calculated accurately into subfactors, giving the soil loss calculation additional flexibility. Through sediment mobility, it is also possible to estimate deposition (McCool et al., 2004). For example, the RUSLE has witnessed significant advancements, particularly in the LS factor, which have revolutionised its applicability on wider scales. In fact, these improvements have facilitated its utilisation even at a global scale (Naipal et al., 2015). Because of this, it has a wide range of applications because of its accessibility to data and simplicity (Balasubramani et al., 2015; Jiang

et al., 2015). RUSLE can compute and estimate the data to determine how much soil has been lost on the basin's valley side. Sedimentation of the river basin and the reservoirs may be evaluated using the RUSLE model's output. The RUSLE model may be used to assess soil loss for river basins, individual farm fields or other areal units.

Additionally, despite its remarkable progress, the challenges in soil erosion modelling persist due to the scarcity of long-term and precise data. Moreover, because the basis of this model is a coefficient that is calibrated based on the data, RUSLE cannot measure the true picture of soil erosion. It is noteworthy that these uncertainties are not exclusive to RUSLE applications but are particularly pronounced in complex models that require extensive data inputs (de Vente & Poesen, 2005; Hernandez et al., 2012).

Despite its relative simplicity and lower data needs, the RUSLE holds the distinction of being the first attempt to estimate soil loss for a landscape, according to Aksoy & Kavvas (2005). However, one of the limitations of the RUSLE is that it solely takes into consideration soil loss attributed to sheet and rill erosion, overlooking the impacts of gully erosion and dispersive soils, which are important factors to consider in soil erosion models and conservation practices (Rowlands, 2019).

The limitations of the model highlighted in previous research (Desmet & Govers, 1996; Wischmeier & Smith, 1958) include the failure to consider deposition or sediment channelling, leading to potential overestimation. However, the implications of these shortcomings extend beyond mere inaccuracies, as they hinder our ability to thoroughly examine downstream regions' susceptibility to anthropogenic activities and sedimentation. This deficiency is due to the model's inability to forecast the paths through which sediment travels from hillslopes to water bodies, as pointed out by Jahun et al. (2015). Moreover, these limitations further restrict the model's ability to depict topographically intricate terrains, as previous studies have indicated.

Despite the acknowledged limitations, the RUSLE family of models continues to be widely utilised due to its inherent advantages of being relatively simple to implement and requiring minimal data compared to more complex physically based models. This model is restricted to a long-term rainfall record and only applies to arable land. In order to accurately assess the impact of rainfall erosion, it is highly recommended

to conduct field measurements, specifically through direct measurements obtained from simulated rainfall. For the purpose of calculating the yearly soil loss, the RUSLE model uses physical characteristics and surface dynamic changes such as the R factor, P factor, K factor, LS factor and C factor. Furthermore, the RUSLE's improved flexibility makes it possible to anticipate soil erosion for various watershed management options and a wider range of ecosystems. This global approach not only ensures continuous improvement but also fosters a deeper understanding of the model's adaptability in varying conditions, making it a valuable tool in studying erosion and soil losses worldwide.

The RUSLE family of models is nevertheless commonly employed in spite of these shortcomings because of its relative simplicity and minimal data needs as compared to more complicated physically based models. These models, developed by Wischmeier and Smith in the 1960s, provide a practical framework for predicting soil erosion rates. While they may lack the fine-grained accuracy and specificity demonstrated by more sophisticated models, the RUSLE family remains a valuable tool for a wide range of users. Moreover, RUSLE provides valuable information about various locales, cropping methods and crops, as well as about erosion in forests and rangelands. Its ease of use and low data requirements make it accessible to researchers, land managers, policymakers and educators alike. Its widespread adoption speaks to its enduring practicality and versatile application. Since soil erosion has increased in frequency and intensity, additional research, better legislation and mitigating measures are necessary. Accordingly, RUSLE parameterisation and application in various climatic regimes and locales are still being improved through studies conducted all over the world.

Conclusion

The problem of erosion addressed through the RUSLE, coupled with GIS, is easily applied thanks to its compatibility with the algebra of maps. GIS allows efficient management of a set of spatially referenced data from the different agents responsible for soil degradation in order to assess the impact of the main factors on water erosion. The results obtained by the application of the RUSLE model are relatively very reliable and constitute a valuable asset at very low

cost, dedicated to managers and decision-makers to target areas at risk. This is done on the basis of simulation models of soil loss evolution scenarios in order to take the necessary and appropriate conservation actions for the fight against erosion.

Finally, it is believed that this work has been able to achieve its main objective with regard to the assessment, at the scale of a watershed, of potential erosion rates and the identification of areas exposed to different degrees of erosion risk by specifying the main factors responsible for soil degradation. Apart from its universal use and reliability, it turns out that the model applied in this study is a fundamental tool for the spatial–temporal assessment of erosion risks. However, it requires continuous updating and refreshing of source data to arrive at results that can help decision-making. The results obtained, in cartographic form, are crucial to locating the sensitive areas exposed to the risks of water erosion, which require priority intervention and appropriate solutions to protect the natural environment.

Author contribution All authors contributed to the study topic and research. Material preparation, data collection and analysis were performed by Okba Weslati and Mohamed Moncef Serbaji. The first draft of the manuscript was written by Okba Weslati. The first written draft of the manuscript was reviewed and corrected by Mohamed Moncef Serbaji. All authors read and approved the final manuscript.

Data availability Please address to Okba Weslati (okba.weslati@gmail.com) for data request.

Declarations

Ethical approval Not applicable.

Competing interests The authors declare no competing interests.

References

Adornado, H. A., Yoshida, M., & Apolinares, H. A. (2009). Erosion vulnerability assessment in REINA, Quezon Province, Philippines with raster-based tool built within GIS environment. *Agricultural Information Research, 18*(1), 24–31. https://doi.org/10.3173/air.18.24

Aiello, A., Adamo, M., & Canora, F. (2015). Remote sensing and GIS to assess soil erosion with RUSLE3D and USPED at river basin scale in southern Italy. *Catena, 131*, 174–185. https://doi.org/10.1016/j.catena.2015.04.003

Aksoy, H., & Kavvas, M. L. (2005). A review of hillslope and watershed scale erosion and sediment transport models.

CATENA, 64(2–3), 247–271. https://doi.org/10.1016/j.catena.2005.08.008

Allafta, H., & Opp, C. (2022). Soil erosion assessment using the RUSLE model, Remote Sensing, and GIS in the Shatt Al-Arab Basin (Iraq-Iran). *Applied Sciences, 12*(15), 7776. https://doi.org/10.3390/app12157776

Almagro, A., Thomé, T. C., Colman, C. B., Pereira, R. B., Marcato Junior, J., Rodrigues, D. B. B., & Oliveira, P. T. S. (2019). Improving cover and management factor (C-factor) estimation using remote sensing approaches for tropical regions. *International Soil and Water Conservation Research, 7*(4), 325–334. https://doi.org/10.1016/j.iswcr.2019.08.005

Anache, J. A. A., Bacchi, C. G. V., Panachuki, E., & Alves Sobrinho, T. (2015). Assessment of methods for predicting soil erodibility in soil loss modeling. *Geociencias, 34*(1), 32–40.

BACC, I., & Team, A. (Eds.). (2015). Second assessment of climate change for the Baltic Sea basin. SpringerOpen. http://link.springer.com/10.1007/978-3-319-16006-1

Bagherzadeh, A. (2014). Estimation of soil losses by USLE model using GIS at Mashhad plain, Northeast of Iran. *Arabian Journal of Geosciences, 7*(1), 211–220. https://doi.org/10.1007/s12517-012-0730-3

Balasubramani, K., Veena, M., Kumaraswamy, K., & Saravanabavan, V. (2015). Estimation of soil erosion in a semi-arid watershed of Tamil Nadu (India) using Revised Universal Soil Loss Equation (RUSLE) model through GIS. *Modeling Earth Systems and Environment, 1*(3), 10. https://doi.org/10.1007/s40808-015-0015-4

Belloula, M., & Dridi, H. (2015). Modeling of the flows and solid transport in the catchment area of Meskiana-Mellegue upstream (Northeastern Algeria). *Geographia Technica, 10*(1), 1–7.

Belloula, M. (2017). *Evaluation de l'aptitude aux écoulements et risque d'érosion dans le haut cours de la Medjerda par Modélisation*. Doctorat thesis, Institut des sciences de la terre et de l'univers. Université de Batna 2.

Benavidez, R., Jackson, B., Maxwell, D., & Norton, K. (2018). A review of the (Revised) Universal Soil Loss Equation ((R)USLE): With a view to increasing its global applicability and improving soil loss estimates. *Hydrology and Earth System Sciences, 22*(11), 6059–6086. https://doi.org/10.5194/hess-22-6059-2018

Beretta-Blanco, A., & Carrasco-Letelier, L. (2017). Factores K de USLE/RUSLE asignados a través de un modelo lineal mixto a suelos de Uruguay. *Ciencia e Investigacion Agraria, 44*(1), 100–112. https://doi.org/10.7764/rcia.v44i1.1622

Biswas, A. K. (1990). Watershed management. *International Journal of Water Resources Development, 6*(4), 240–249. https://doi.org/10.1080/07900629008722479

Houssem Braiki. (2018). Construction d'une démarche participative pour améliorer la gestion de l'eau et du sol. Une application aux politiques des aménagements de conservation des eaux et des sols en Tunisie Centrale. Environnement et Société. AgroParisTech; Institut national agronomique de Tunisie, 2018. NNT : 2018AGPT0003ff. tel-01960275v2f.

Cherni, S., Khlifi, S., & Louati, M. H. (2010). SUIVI DE L'ENVASEMENT DE LA RETENUE DU BARRAGE DE NEBEUR SUR L'OUED MELLEGUE (LE KEF).

Conference In *Actes des 17èmes Journées Scientifiques sur les Résultats de la Recherche Agricoles*.

Chriha, S., & Sghari, A. (2013). Forest fires in Tunisia, irreversible sequelae of the revolution of 2011. *Journal of Mediterranean Geography, 121*.

Ciampalini, R., Follain, S., & Le Bissonnais, Y. (2012). LandSoil: A model for analysing the impact of erosion on agricultural landscape evolution. *Geomorphology, 175–176*, 25–37. https://doi.org/10.1016/j.geomorph.2012.06.014

Cooper, M. (2010). Advanced Bash-Scripting Guide An in-depth exploration of the art of shell scripting Table of Contents. *Okt 2005 Abrufbar uber httpwww tldp orgLDPabsabsguide pdf Zugriff 1112 2005, 2274*(November 2008), 2267–2274. https://doi.org/10.1002/hyp

David, W. P. (1988). Soil and Water conservation planning: Policy issues and recommendations. *Journal of Philippine Development, 15*(1), 47–84.

De Jong, S. M., Paracchini, M. L., Bertolo, F., Folving, S., Megier, J., & De Roo, A. P. J. (1999). Regional assessment of soil erosion using the distributed model SEMMED and remotely sensed data. *Catena, 37*(3–4), 291–308. https://doi.org/10.1016/S0341-8162(99)00038-7

de Vente, J., & Poesen, J. (2005). Predicting soil erosion and sediment yield at the basin scale: Scale issues and semi-quantitative models. *Earth-Science Reviews, 71*(1–2), 95–125. https://doi.org/10.1016/j.earscirev.2005.02.002

Desmet, P. J. J., & Govers, G. (1996). A GIS Procedure for Automatically Calculating the USLE LS Factor on Topographically Complex Landscape Units. *Journal of Soil and Water Conservation, 51*, 427–433.

Durán Zuazo, V. H., Aguilar Ruiz, J., Martínez Raya, A., & Franco Tarifa, D. (2005). Impact of erosion in the taluses of subtropical orchard terraces. *Agriculture, Ecosystems and Environment, 107*(2–3), 199–210. https://doi.org/10.1016/j.agee.2004.11.011

Durigon, V. L., Carvalho, D. F., Antunes, M. A. H., Oliveira, P. T. S., & Fernandes, M. M. (2014). NDVI time series for monitoring RUSLE cover management factor in a tropical watershed. *International Journal of Remote Sensing, 35*(2), 441–453. https://doi.org/10.1080/01431161.2013.871081

Elbouqdaoui, K., Ezzine, H., Badrahoui, M., Rouchdi, M., Zahraoui, M., & Ozer, A. (2005). Approche méthodologique par télédétection et SIG de l'évaluation du risque potentiel d'érosion hydrique dans le bassin versant de l'Oued Srou (Moyen Atlas, Maroc). *Geo-Eco-Trop, 29*(1–2), 25–36.

Latham, M. (1981). The FAO/UNESCO soil map of the world legend. In *South Pacific Regional Forum on Soil Taxonomy* (pp. 177–183). Institute of Natural Resources, The University of the South Pacific Suva, Fiji.

Fehri, N. (2014). L'aggravation du risque d'inondation en Tunisie : éléments de réflexion. *Physio-Géo, Volume 8*, 149–175. https://doi.org/10.4000/physio-geo.3953

Gebregziabher, G., Abera, D. A., Gebresamuel, G., Giordano, M., & Langan, S. (2016). An assessment of integrated watershed management in Ethiopia. Colombo, Sri Lanka: International Water Management Institute (IWMI). (IWMI Working Paper 170, p. 28). https://doi.org/10.5337/2016.214

Gilley, J. E. (2005). EROSION/Water-Induced. *Encyclopedia of Soils in the Environment* (pp. 463–469). https://doi.org/10.1016/B0-12-348530-4/00262-9

Goumrasa, A., Guendouz, M., Guettouche, M. S., Akziz, D., & Bouguerra, H. (2021). Spatial assessment of water erosion hazard in Chiffa wadi watershed and along the first section of the Algerian North-South highway using remote sensing data, RUSLE, and GIS techniques. *Arabian Journal of Geosciences, 14*(20), 2152. https://doi.org/10.1007/s12517-021-08377-5

Guerra, A. (1994). The effect of organic matter content on soil erosion in simulated rainfall experiments in W. Sussex, UK. *Soil Use and Management, 10*(2), 60–64. https://doi.org/10.1111/j.1475-2743.1994.tb00460.x

Hernandez, E. C., Henderson, A., & Oliver, D. P. (2012). Effects of changing land use in the Pagsanjan-Lumban catchment on suspended sediment loads to Laguna de Bay, Philippines. *Agricultural Water Management, 106*, 8–16. https://doi.org/10.1016/j.agwat.2011.08.012

Jahun, B. G., Ibrahim, R., Dlamini, N. S., & Musa, S. M. (2015). Review of soil erosion assessment using RUSLE Model and GIS. *Journal of Biology, Agriculture and Healthcare, 5*(9), 36–47.

Jiang, L., Yao, Z., Liu, Z., Wu, S., Wang, R., & Wang, L. (2015). Estimation of soil erosion in some sections of Lower Jinsha River based on RUSLE. *Natural Hazards, 76*(3), 1831–1847. https://doi.org/10.1007/s11069-014-1569-6

Karaburun, A. (2010). Estimation of C factor for soil erosion modeling using NDVI in Buyukcekmece watershed. *Ozean Journal of Applied Sciences, 3*(1), 77–85. http://ozelacademy.com/OJAS_v3n1_8.pdf

Kebede, Y. S., Endalamaw, N. T., Sinshaw, B. G., & Atinkut, H. B. (2021). Modeling soil erosion using RUSLE and GIS at watershed level in the upper beles, Ethiopia. *Environmental Challenges, 2*, 100009. https://doi.org/10.1016/j.envc.2020.100009

Khanchoul, K., Selmi, K., & Benmarce, K. (2020). Assessment of Soil Erosion By Rusle Model in the Mellegue Watershed, Northeast of Algeria. *Environment & Ecosystem Science, 4*(1), 15–22. https://doi.org/10.26480/ees.01.2020.15.22

Khemiri, K., & Jebari, S. (2021). Évaluation de l'érosion hydrique dans des bassins versants de la zone semi-aride tunisienne avec les modèles RUSLE et MUSLE couplés à un Système d'information géographique. *Cahiers Agricultures, 30*, 7. https://doi.org/10.1051/cagri/2020048

Kinnell, P. I. A. (2010). Event soil loss, runoff and the universal soil loss equation family of models: A review. *Journal of Hydrology, 385*(1–4), 384–397. https://doi.org/10.1016/j.jhydrol.2010.01.024

Kulikov, M., Schickhoff, U., & Borchardt, P. (2016). Spatial and seasonal dynamics of soil loss ratio in mountain rangelands of south-western Kyrgyzstan. *Journal of Mountain Science, 13*(2), 316–329. https://doi.org/10.1007/s11629-014-3393-6

Littleboy, M., Freebaim, D. M., Hammer, G. L., & Silbum, D. M. (1992). Impact of soil erosion on production in cropping systems. II.* Simulation of production and erosion risks for a wheat cropping system. *Australian Journal of*

Soil Research, 30(5), 775–788. https://doi.org/10.1071/SR9920775

López-Bermúdez, F. (1990). Soil erosion by water on the desertification of a semi-arid Mediterranean fluvial basin: The Segura basin, Spain. *Agriculture, Ecosystems and Environment, 33*(2), 129–145. https://doi.org/10.1016/0167-8809(90)90238-9

Mahleb, A., Hadji, R., Zahri, F., Boudjellal, R., Chibani, A., & Hamed, Y. (2022). Water-borne erosion estimation using the Revised Universal Soil Loss Equation (RUSLE) model over a semiarid watershed: Case study of Meskiana Catchment, Algerian-Tunisian Border. *Geotechnical and Geological Engineering, 40*(8), 4217–4230. https://doi.org/10.1007/s10706-022-02152-3

Mammou, A. B., & Louati, M. H. (2007). Évolution temporelle de l'envasement des retenues de barrages de Tunisie. *Revue Des Sciences De L'eau, 20*(2), 201–210. https://doi.org/10.7202/015813ar

Martínez-Murillo, J. F., Remond, R., & Ruiz-Sinoga, J. D. (2020). Validation of RUSLE K factor using aggregate stability in contrasted mediterranean eco-geomorphological landscapes (southern Spain). *Environmental Research, 183*(January), 109160. https://doi.org/10.1016/j.envres.2020.109160

McCool, D. K., Foster, G. R., Yoder, D. C., & Weesies, G. A. (2004). The revised universal soil loss equation, Version 2. In: International Soil Conservation Organization Conference Proceedings

Mitasova, H., Hofierka, J., Zlocha, M., & Iverson, L. R. (1996). Modelling topographic potential for erosion and deposition using GIS. *International Journal of Geographical Information Systems, 10*(5), 629–641. https://doi.org/10.1080/02693799608902101

Mohanty, A. (2016). Sustainable Watershed Management Afghanistan: a case study of Agriculture Kahmard District. Conference on National Seminar In *Agriculture Crisis and Goverence in India : Issues and Concerns , New Delhi, 2016.*

Morgan, R. P. C. (2005). Soil Erosion and Conservation (3rd ed.). John Wiley & Sons.

Mounirou, L. A. (2012). Etude du ruissellement et de l'érosion à différentes échelles spatiales sur le bassin versant de Tougou en zone sahélienne du Burkina Faso : quantification et transposition des données. Thesis. Université Montpellier II.

Naipal, V., Reick, C., Pongratz, J., & Van Oost, K. (2015). Improving the global applicability of the RUSLE model—adjustment of the topographical and rainfall erosivity factors. *Geoscientific Model Development, 8*(9), 2893–2913. https://doi.org/10.5194/gmd-8-2893-2015

Negese, A. (2021). Impacts of Land use and land cover change on soil erosion and hydrological responses in Ethiopia. *Applied and Environmental Soil Science, 2021*, 15–17. https://doi.org/10.1155/2021/6669438

Nord, G. (2006). *Modélisation à base physique des processus de l ' érosion hydrique à l ' échelle de la parcelle*. Université Joseph-Fourier- Grenoble I.

Nunes, A. N., Coelho, C. O. A., De Almeida, A. C., & Figueiredo, A. (2010). Soil erosion and hydrological response to land abandonment in a central inland area of Portugal.

Land Degradation and Development, 21(3), 260–273. https://doi.org/10.1002/ldr.973

Ostertagová, E. (2012). Modelling using polynomial regression. *Procedia Engineering, 48*(December 2012), 500–506. https://doi.org/10.1016/j.proeng.2012.09.545

Pavlova-traykova, E. (2020). Evaluation of water erosion risk in Bistritsa river watershed , south-west Bulgaria. *Forest Science (0861-007X), 55*(1), 53–63.

Prosdocimi, M., Cerdà, A., & Tarolli, P. (2016). Soil water erosion on Mediterranean vineyards: A review. *Catena, 141*, 1–21. https://doi.org/10.1016/j.catena.2016.02.010

Raclot, D., Le Bissonnais, Y., Annabi, M., Sabir, M., & Smetanova, A. (2018). Main Issues for Preserving Mediterranean Soil Resources From Water Erosion Under Global Change. *Land Degradation and Development, 29*(3), 789–799. https://doi.org/10.1002/ldr.2774

Rawat, K. S., & Singh, S. K. (2018). Appraisal of soil conservation capacity using NDVI model-based C factor of RUSLE Model for a semi arid ungauged watershed: A case study. *Water Conservation Science and Engineering, 3*(1), 47–58. https://doi.org/10.1007/s41101-018-0042-x

Renard, K., Foster, G., Weesies, G., McCool, D., & Yoder, D. (1997). *Predicting soil erosion by water: a guide to conservation planning with the Revised Universal Soil Loss Equation (RUSLE)*. US Department of Agriculture, Agriculture Handbook No.703USDA, USDA, Washington DC.

Rodier, J. A., Colombani, J., Claude, J., & Kallel, R. (1981). ORSTOM, p. 451. https://www.worldcat.org/title/bassin-de-la-mejerdah/oclc/469086740

Rouvier, H. (1977). Géologie de l'extrême nord-tunisien: tectonique et paléogéographie superposées à l'extrémité orientale de la chaine nord-maghrébine. Doctoral dissertation, Ed. du Service géologique de Tunisie.

Rowlands, L. (2019). Erosion and Sediment Control—WSUD During the construction phase of land development. In *Approaches to Water Sensitive Urban Design* (pp. 163–176). Elsevier. https://doi.org/10.1016/B978-0-12-812843-5.00008-3

Sadiki, A., Bouhlassa, S., Auajjar, J., Faleh, A., & Macaire, J.-J. (2004). Utilisation d'un SIG pour l'évaluation et la cartographie des risques d'érosion par l'Equation universelle des pertes en sol dans le Rif oriental (Maroc): cas du bassin versant de l'oued Boussouab. *Bulletin de l'Institut Scientifique, Rabat, section Sciences de la Terre, 26*(December 2015), 69–79.

Sahar, A., Olfa, H., Ezzine, A., & Hermassi, T. (2019). Cartographie du risque d' inondation de la Haute Vallée de Medjerda avec Hec- Ras. *Journal International Sciences et Technique de l'Eau et de l'Environnement (JISTEE), 4.*

Sbai, A., Mouadili, O., Hlal, M., Benrbia, K., Zahra Mazari, F., Bouabdallah, M., & Saidi, A. (2021). Water erosion in the Moulouya Watershed and its impact on dams' siltation (Eastern Morocco). *Proceedings of the International Association of Hydrological Sciences, 384*, 127–131. https://doi.org/10.5194/piahs-384-127-2021

Schmitt, L. K. (2009). Developing and applying a soil erosion model in a data-poor context to an island in the rural Philippines. *Environment, Development and Sustainability, 11*(1), 19–42. https://doi.org/10.1007/s10668-007-9096-1

Serbaji, M. M., Bouaziz, M., & Weslati, O. (2023). Soil water erosion modeling in Tunisia using RUSLE and GIS integrated approaches and geospatial data. *Land, 12*(3), 548. https://doi.org/10.3390/land12030548

Sergieieva, K. (2021). Water erosion: types, causes, effects, and prevention. EOS Data Analytics (*Eos.com*). https://eos.com/blog/water-erosion/

Shalaby, A., & Tateishi, R. (2007). Remote sensing and GIS for mapping and monitoring land cover and land-use changes in the Northwestern coastal zone of Egypt. *Applied Geography, 27*(1), 28–41. https://doi.org/10.1016/j.apgeog.2006.09.004

Shin, G. J. (1999). The Analysis of Soil Erosion Analysis in Watershed Using GIS. *Ph.D. Dissertation, Department of Civil Engineering, Gang-Won National University, Chuncheon.*

Sidi Almouctar, M. A., Wu, Y., Zhao, F., & Dossou, J. F. (2021). Soil erosion assessment using the RUSLE Model and Geospatial Techniques (Remote Sensing and GIS) in South-Central Niger (Maradi Region). *Water, 13*(24), 3511. https://doi.org/10.3390/w13243511

Singh, A. (1989). Review Article: Digital change detection techniques using remotely-sensed data. *International Journal of Remote Sensing, 10*(6), 989–1003. https://doi.org/10.1080/01431168908903939

Starr, G. C., Lal, R., Malone, R., Hothem, D., Owens, L., & Kimble, J. (2000). Modeling soil carbon transported by water erosion processes. *Land Degradation and Development, 11*(1), 83–91. https://doi.org/10.1002/(SICI)1099-145X(200001/02)11:1%3c83::AID-LDR370%3e3.0.CO;2-W

Thapa, P. (2020). Spatial estimation of soil erosion using RUSLE modeling: A case study of Dolakha district, Nepal. *Environmental Systems Research, 9*(1), 15. https://doi.org/10.1186/s40068-020-00177-2

Touai'bia, B., Gomer, D., & Aïdaoui, A. (1999). Estimation De L'index D'erosion De Wischmeier Dans Les Micro Bassins Experimentaux De L'oued Mina En Algerie Du Nord. In *Bulletin du Réseau Érosion, 20*, 478–484.

Vaezi, A. R., & Sadeghi, S. H. R. (2011). Evaluating the RUSLE model and developing an empirical equation for estimating soil erodibility factor in a semi-arid region. *Spanish Journal of Agricultural Research, 9*(3), 912. https://doi.org/10.5424/sjar/20110903-229-10

van der Knijff, J. M., Jones, R. J. A., & Montanarella, L. (2000). European soil erosion risk assessment. European Soil Bureau. EUR 19044 EN, pp. 34. https://esdac.jrc.ec.europa.eu/content/soil-erosion-risk-assessment-europe

Vezina, K., Bonn, F., & Van, C. P. (2006). Agricultural land-use patterns and soil erosion vulnerability of watershed units in Vietnam's northern highlands. *Landscape Ecology, 21*(8), 1311–1325. https://doi.org/10.1007/s10980-006-0023-x

Wang, R., Li, P., Li, Z., Yu, K., Han, J., Zhu, Y., & Su, Y. (2021). Effects of gully head height and soil texture on gully headcut erosion in the Loess Plateau of China.

CATENA, 207, 105674. https://doi.org/10.1016/j.catena.2021.105674

Wasswa, P., & Olilla, D. (2006). An empirical approach to estimate soil erosion and its correlation with landslide events (a case study from Vazroud watershed, N Iran). *African Journal of Traditional, Complementary and Alternative Medicines, 3*(2), 94–103.

Weslati, O., Bouaziz, S., & Serbaji, M. M. (2020). Mapping and monitoring land use and land cover changes in Mellegue watershed using remote sensing and GIS. *Arabian Journal of Geosciences, 13*, 687. https://doi.org/10.1007/s12517-020-05664-5

Weslati, O., Bouaziz, S., & Sarbeji, M. M. (2023). Modelling and Assessing the Spatiotemporal Changes to Future Land Use Change Scenarios Using Remote Sensing and CA-Markov Model in the Mellegue Catchment. *Journal of the Indian Society of Remote Sensing, 51*, 9–29. https://doi.org/10.1007/s12524-022-01618-4

Wischmeier, W. H., & Smith, D. D. (1958). Rainfall energy and its relationship to soil loss. *Transactions, American Geophysical Union, 39*(2), 285. https://doi.org/10.1029/TR039i002p00285

Wuepper, D., Borrelli, P., & Finger, R. (2019). Countries and the global rate of soil erosion. *Nature Sustainability, 3*(1), 51–55. https://doi.org/10.1038/s41893-019-0438-4

Yan, H., Wang, L., Wang, T. W., Wang, Z., & Shi, Z. H. (2020). A synthesized approach for estimating the C-factor of RUSLE for a mixed-landscape watershed: A case study in the Gongshui watershed, southern China. *Agriculture, Ecosystems and Environment, 301*(March), 107009. https://doi.org/10.1016/j.agee.2020.107009

Zema, D. A., Carrà, B. G., Lucas-Borja, M. E., Filianoti, P. G. F., Pérez-Cutillas, P., & Conesa-García, C. (2022). Modelling water flow and soil erosion in mediterranean headwaters (with or without check dams) under land-use and climate change scenarios using SWAT. *Water, 14*, 2338. https://doi.org/10.3390/w14152338

Zhao, W. W., Fu, B. J., & Chen, L. D. (2012). A comparison between soil loss evaluation index and the C-factor of RUSLE: A case study in the Loess Plateau of China. *Hydrology and Earth System Sciences, 16*(8), 2739–2748. https://doi.org/10.5194/hess-16-2739-2012